

# POSITIONING THE ZETA FUNCTION ZEROS WITHIN AN OPTIMUM FRAME OF REFERENCE

HUBERT SCHAETZEL

**ABSTRACT.** The purpose of this article is to design a frame of reference enabling to locate the Zeta function zeros with the smallest margin of error. This optimal frame, based on a constant real part, favours the spring of some most interesting properties of these zeros, partial zeros pairings, Gaussian distributions, identification of uncommon permutations of positions...

**RÉSUMÉ.** (*Positionner les zéros de la fonction Zêta de Riemann dans un système de référence optimal*).

Le but de cet article est de bâtir un repère permettant de positionner les zéros de la fonction Zêta de façon la plus précise possible. Ce repère optimal, basé sur une partie réelle constante, favorise l'émergence de propriétés intéressantes de ces zéros, appariements à des zéros partiels, distributions gaussiennes, identification d'inhabituelles permutations de positions...

## CONTENTS

|  |    |
|--|----|
| 1. Introduction                                | 2  |
| 2. Short return to the Riemann hypothesis      | 3  |
| 3. The pain-free locus                         | 7  |
| 4. Defining the appropriate frame of reference | 8  |
| 5. The pairing of cancellations                | 9  |
| 6. Gaussian distributions                      | 11 |
| 7. Shifting of ordinates                       | 14 |
| 8. Sinusoidal birth of curves                  | 15 |
| 9. The imaginary domain is a stronghold        | 18 |
| 10. The partial cancellations' network         | 19 |
| 11. Conclusion                                 | 27 |
| Appendix A. Conformal maps                     | 28 |
| Appendix B. Partial Zeta zeros                 | 32 |
| Appendix C. Graphics of deviations             | 33 |
| Appendix D. Data of standard deviations        | 35 |

---

*Date:* March 18, 2023.

*2020 Mathematics Subject Classification.* 11M26, 30C35.

*Key words and phrases.* Riemann hypothesis, conformal map, Lambert W function, Gaussian distribution.

|  |    |
|--|----|
| Appendix E. Proportion of consecutive sequences of zeros | 36 |
| Appendix F. Three consecutive zeros                      | 37 |
| Appendix G. Pari gp programs                             | 46 |
| Literature and sources                                   | 47 |

## 1. INTRODUCTION

The Riemann Zeta function is defined over the complex plane  $Re(s) > 1$  by

$$\zeta(s) = \sum_{n=1}^{\infty} \frac{1}{n^s}$$

This function has an analytic continuation over the whole complex plane except the unique complex point  $s = 1 + 0.i$ . The Riemann's hypothesis, formulated in 1859 [1], is that the non-trivial zeros of the function are such that  $Re(s) = \frac{1}{2}$ , the zeros quoted as trivial being  $s = -2n$ ,  $n \in \mathbb{N}^*$ .

A well-established result is that all the non-trivial zeros are located within the critical band  $0 \leq Re(s) \leq 1$ . In search of zeros, one can reduce the review to the domain  $0 \leq \alpha \leq 1/2$  thanks to the following fact:

**Theorem 1.** *Within the critical band, the non-trivial  $\zeta$ -function zeros are symmetrical to the axis  $s = 1/2$ .*

*Proof.* Using the functional equation (see [2])

$$\zeta(s) = 2^s \pi^{s-1} \sin \frac{\pi s}{2} \Gamma(1-s) \zeta(1-s),$$

Let us write then  $\xi(s) = (1/2)\pi^{-s/2}s(s-1)\Gamma(s/2)\zeta(s)$ . Referring to [10], we get immediately  $\xi(s) = \xi(1-s)$ .  $\square$

Therefore looking for exception to the Riemann rule is equivalent to examine the  $\{0 \leq s < 1/2\}$  cases.

As a meromorphic function [10], the Zeta function is infinitely derivable except at its pole. The previous theorem then extends to its derivatives:

**Theorem 2.** *Within the critical band, the non-trivial systematic multiple zeros of the  $\zeta$ -function are symmetrical to the axis  $s = 1/2$ .*

*Proof.* We refer to [3] which provides the functional equation of the  $k^{th}$  derivative of  $\zeta(s)$

$$(-1)^k \zeta^{(k)}(1-s) = 2(2\pi)^{-s} \sum_{j=0}^k \sum_{m=0}^k (a_{jkm} \cos \frac{\pi s}{2} + b_{jkm} \sin \frac{\pi s}{2}) \Gamma^{(j)}(s) \zeta^{(m)}(s).$$

Thus  $\zeta^{(k)}(1-s) = 0$  if  $\zeta^{(m)}(s) = 0$  for each  $m = 0$  to  $k$ . Hence the symmetry with respect to the axis  $s = 1/2$  at step  $k$  for a systematic multiple zero up to  $k$ .  $\square$

To study the  $\zeta$ -function, one can use the Euler-Maclaurin formula, an integral on  $\mathbb{R}^+$ , a contour integral in the  $C$  plane or the Abel sum, this list not being exhaustive [10]. The said function is available on online platforms. The Pari gp application, chosen here whenever we wish to provide some numerical illustrations, usually uses the Euler-Maclaurin formula, unless integers are involved in which case the use of Bernoulli numbers or modular forms is activated (see User guide to Pari gp).

Finding the non-trivial zeros of the  $\zeta$ -function is to solve, within the critical band, simultaneously

$$\operatorname{Re}(\zeta(s)) = 0 \quad \text{and} \quad \operatorname{Im}(\zeta(s)) = 0$$

where  $\operatorname{Re}(\zeta(s))$  designates the real part of  $\zeta(s)$  and  $\operatorname{Im}(\zeta(s))$  is its imaginary part.

The purpose of this article is to find an adequate set to locate the solutions to the two equations. It seems almost obvious, short of its effective relevance, to choose a priori the two sets:

$$\text{Set 2 : } \{ \operatorname{Re}(\zeta(s)) = 0 \text{ and } \operatorname{Im}(\zeta(s)) \neq 0 \} \quad (1)$$

$$\text{Set 3 : } \{ \operatorname{Re}(\zeta(s)) \neq 0 \text{ and } \operatorname{Im}(\zeta(s)) = 0 \} \quad (2)$$

The locus of the  $n^{\text{th}}$  Riemann zeros is addressed by the standard coordinates setting  $\sigma_n + i \cdot t_n$ . For the set  $\{ \operatorname{Re}(\zeta(s)) = 0 \text{ and } \operatorname{Im}(\zeta(s)) \neq 0 \}$ , we will use  $\sigma r_n + i \cdot t r_n$ , while for  $\{ \operatorname{Re}(\zeta(s)) \neq 0 \text{ and } \operatorname{Im}(\zeta(s)) = 0 \}$ , we will spot the elements with  $\sigma i_n + i \cdot t i_n$ :

$$\begin{aligned} \text{Set 1 : } \operatorname{Re}(\zeta(s)) = 0 \text{ and } \operatorname{Im}(\zeta(s)) = 0 &\Leftrightarrow s = \sigma_n + i \cdot t_n \\ \text{Set 2 : } \operatorname{Re}(\zeta(s)) = 0 \text{ and } \operatorname{Im}(\zeta(s)) \neq 0 &\Leftrightarrow s = \sigma r_n + i \cdot t r_n \\ \text{Set 3 : } \operatorname{Re}(\zeta(s)) \neq 0 \text{ and } \operatorname{Im}(\zeta(s)) = 0 &\Leftrightarrow s = \sigma i_n + i \cdot t i_n \end{aligned}$$

Given some coordinate  $s$  value, we will also call, here and there,  $\sigma$  the abscissa and  $t$  the ordinate.

## 2. SHORT RETURN TO THE RIEMANN HYPOTHESIS

**Lemma 1.** *The non-trivial zeros of the Zeta function are all located on the critical line except eventually in the case of some double zero  $s$ , that is if  $\zeta(s) = \zeta'(s) = 0$  (and  $\sigma \neq 1/2$ ).*

*Proof.* One of the property of an analytic function is the conservation of angles [6] [15] wherever the derivative doesn't cancel.

So let us consider a rectangle  $r$  in the complex plane not encompassing the pole (1,0) of the function, this later case being considered in appendix A. Applying the function to the rectangle  $r$ , the resulting figure  $\zeta(r)$  will be a deformed "rectangle". If the rectangle is small, the resulting conformal map [15] is a quasi-rectangle. Local deformation results from non-null scaling factors. The trajectories of the opposite sides of the initial rectangle will give local "parallel" trajectories of the images in the complex plane. Corresponding opposite points of same abscissa, or of same ordinate, don't meet

in the image because of the non-null scaling.

A typical example of rectangle deformation is given in figure 1. Of course, as the figure shows, if the rectangle gets long enough, part of the image set can overlap. To get a bijection, an artefact would be to add the depth's dimension (for example attribute to this extra coordinate the value of the length along the red line starting at the bottom left vertex), allowing to unfold the image like a Riemann surface. Going back to the complex plane (without additional dimension), the non-null scaling ensures that the red line stays always on the same side of the blue line (as does the yellow line in regard of the green one).

Now, let us consider a rectangle  $r$  centred on the critical axis. Let us choose the rectangle so that the abscissa of a non-trivial zero identified on the lower half of the critical band is on the left side of the said rectangle. By the functional equation, we know the existence of another zero on the right side of the rectangle exactly at the same height, giving the same image  $0 + i.0$ , hence a contradiction with the local bijection.

Of course, to be exhaustive, as said in the first phrase of the argumentation, we have to be sure that no point within the initial rectangle corresponds to a zero of the derivative of Zeta causing some eventual havoc to our argument. If so, one will reduce simply the vertical size of the rectangle  $r$ . The set of real numbers  $\Re$  being dense, this reduction can be as small as needed, the only way to an exception being that this zero of the Zeta function is at the same ordinate as the zero of its derivative. In this peculiar case, one will choose a slightly rounded rectangular shape for the Zeta function's domain, therefore avoiding the zero of the derivative. The conformal map's argument can then be applied without dispute except if the zeros to  $\zeta$ -function and its derivative are the same, the previously mentioned double zero's case.  $\square$

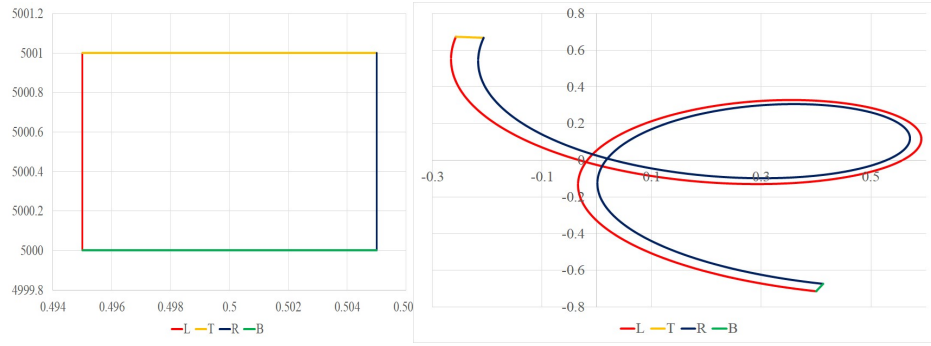
In figure 1, as the chosen initial rectangle is encompassing two solutions  $s$  to  $\zeta(s) = 0$  (the 4521<sup>th</sup> zero equal approximatively to  $1/2 + i.5000.2343169$  and the 4522<sup>th</sup> zero near the complex value  $1/2 + i.5000.8343814$ , we get two transits around the axis intersection.

Remarkable cases like the Zeta function's pole (1,0) and the two first of its trivial zeros (-2,0) and (-4,0), the other trivial zeros being similar, are displayed in appendix A.

*Note.* Although not crucial to our argument, we give some information in appendix A figures 25 *a* and *b* about the pattern in the vicinity of a first derivative's cancelling. In a sufficient close-up, there is no difference to the standard behaviour, a rectangle is still transformed in an almost rectangular surface. But bereft of a proof to generalize this observation, we resolve to the following further analysis.

**Lemma 2.** *The non-trivial zeros of the Zeta function are all located on the critical line except if  $\zeta(s) = \zeta'(s) = \zeta''(s) = \dots \zeta^{(n)}(s) \dots = 0$  for any  $n \in \mathbb{N}^*$  (and  $\sigma \neq 1/2$ ).*

FIGURE 1.  
Initial rectangle  $r$  delimiting  
 $\sigma = [0.495, 0.505]$ ,  $t = [5000, 5001]$   
Image "rectangle"  $\zeta(r)$



*Proof.* The Zeta function is an analytic complex meromorphic function. So it is indefinitely derivable and each derivative is also analytic. The functional expression of the  $n^{th}$  derivative of  $\zeta(s)$  is provided in the proof of theorem 2. According to that general functional equation, if  $\zeta(s) = 0$  and  $\zeta'(s) = 0$  then  $\zeta'(1-s) = 0$ . Then we apply the previous local conformal map's argument to  $\zeta'(s)$  instead of  $\zeta(s)$ . A potential exception is thereafter the case  $\zeta(s) = \zeta'(s) = \zeta''(s) = 0$ . Recalling that the functional equation implies the symmetry with respect to the axis  $s = 1/2$  for systematic multiple zeros and that the conformal map's argument applies to any analytic function, the procedure can be repeated as long as the derivative of the current derivative is null. If not, we get a contradiction to the possibility to have a non-trivial zero outside the critical line.

Hence the non-trivial zeros of the Zeta function not located on the critical line are infinite multiple zeros.  $\square$

Figures 2 and 3 show the examples of deformation of rectangles by the first and second derivatives of the Zeta function. In order to collect these graphics, we use the quotient difference's and the second symmetric derivative's approximations  $(\zeta(s+\Delta\epsilon) - \zeta(s))/\Delta\epsilon$  and  $(\zeta(s+\Delta\epsilon) - 2\zeta(s) + \zeta(s-\Delta\epsilon))/\Delta\epsilon^2$ . The choice of  $\Delta\epsilon$  for these developments is arbitrary as long as small enough. It can be purely real or purely imaginary or a mix. Here the data collection was done with  $\Delta\epsilon = 0.00001$  except for the red curves where we use  $\Delta\epsilon = 0.00001i$  (to show that it has no damaging effect and that the curves still stay "parallel" and meet at their vertices).

In these figures, we observe, here and there, places where the red and blue curves get, for corresponding equal ordinates in the initial rectangle, very near one to each other. However, as we checked on close-ups, there is no meeting (nor therefore crossing) of the two curves.

FIGURE 2.  
Initial rectangle  $r$  delimiting  
 $\sigma = [0.495, 0.505]$ ,  $t = [0.2, 21]$   
Image "rectangle"  $\zeta'(r)$

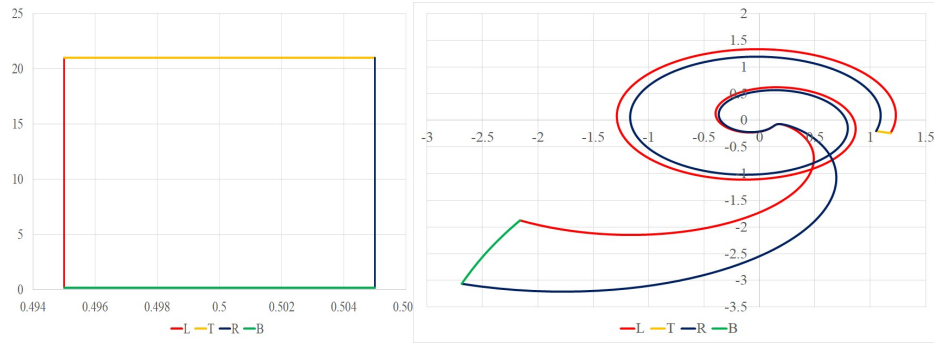
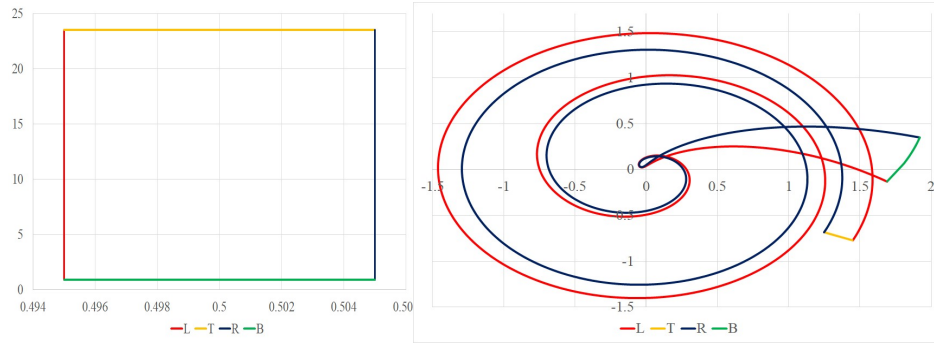


FIGURE 3.  
Initial rectangle  $r$  delimiting  
 $\sigma = [0.495, 0.505]$ ,  $t = [0.9, 23.5]$   
Image "rectangle"  $\zeta''(r)$



*Note.* The reader will find an example of second derivative's cancellation's effect on the first derivative of  $\zeta(s)$  in appendix A figures 26 *a* and *b*. It shows the same pattern as the first derivative's cancellation's effect on  $\zeta(s)$ .

**Theorem 3.** *The non-trivial zeros of the Zeta function are all located on the critical line.*

*Proof.* The Zeta function is a meromorphic [16] function and holomorphic at every point except  $(1,0)$ . Locally at  $\rho$ , its identified  $n^{th}$  multiple zero, it can be written as  $\zeta(s) = \sum_{m \geq n} a_m (s - \rho)^m$  where  $a_m$  are constant complex coefficients. By the previous lemma however, for any finite  $n$ , the coefficients  $a_m$  remain dependant of  $s$  and therefore there is no possible escape to that dependency, thus a contradiction to the property of holomorphy. The Riemann hypothesis is therefore true.  $\square$

This result set forth, let us consider the "trivial" zeros

$$s = 1 + ik \frac{2\pi}{Ln(2)}, \quad k \in \mathbb{Z}, \quad (3)$$

of another analytic continuation of Zeta (over  $Re(s) > 0$ ), built on Dirichlet Eta function, and defined by  $\zeta(s) = (1 - 2^{1-s}) \cdot \eta(s) = (1 - 2^{1-s}) \sum_{n=1}^{\infty} \frac{(-1)^n}{n^s}$ . We observe the obvious constant real part. It happens that the two sets  $\{s = 1 + ik \frac{2\pi}{Ln(2)}\}$  and  $\{s = 1/2 + it\}$  show identical behaviour in graphic representations (see [17] Dirichlet sheet). So, why wouldn't the similarity of the constance of real parts be a hint to some hidden similarity in their imaginary parts? Where has gone the periodicity exposed in equation 3 so acutely? Isn't there still something worth to be dug into? These questions will be addressed soon.

### 3. THE PAIN-FREE LOCUS

The following result was formulated by Bernhard Riemann in 1859 and proven by Hans Carl Friedrich von Mangoldt in 1905 [13]:

**Theorem 4.** *Riemann - von Mangoldt formula: The number  $N(t)$  of zeros of the zeta function with imaginary part greater than 0 and less than or equal to  $t$  satisfies*

$$N(t) = \frac{t}{2\pi} Ln \frac{t}{2\pi} - \frac{t}{2\pi} + O(Ln(t)).$$

where  $Ln()$  is the Napierian logarithm.

Reference [4] provides a proof of a more precise result as  $t \rightarrow \infty$ :

$$N(t) = \frac{t}{2\pi} Ln \frac{t}{2\pi} - \frac{t}{2\pi} - 7/8 + \frac{1}{\pi} \int_{1/2}^{\infty} Im(-\frac{\zeta'}{\zeta}(\sigma + i.t)) d\sigma + O(t^{-1})$$

Let us get then the approximate reciprocal function of  $N(t)$  is order to produce an upper boundary approximation of the locus of the  $n^{th}$  Riemann zero. For that, we use the following theorem.

**Theorem 5.** *The reciprocal function of  $n = T Ln(T) - T + a$ ,  $n$  a function of  $T$ , is given by (refer for example to [5]):*

$$T = \frac{n - a}{W(\frac{n-a}{e})}$$

where  $e = \exp(1)$  and  $W$  is the Lambert function [12] defined by  $w = W(y)$  where  $w.e^w = y$ .

Then some approximate ordinate  $t_n$  of the  $n_{th}$   $\zeta$ -function zero, using the substitution  $t = 2\pi T$ , is provided by

$$t_n \approx 2\pi \frac{n + 7/8 - 2}{W(\frac{n+7/8-2}{e})} \quad (4)$$

where, via a numerical verification, we choose the appropriate beginning index  $n = 1$  and the offset  $-2$  in the  $t_n$  expression for the first Riemann zero approximation.

*Note.* In 1993, it was reported that the Lambert  $W$  function provides an exact solution to the quantum-mechanical double-well Dirac delta function model for equal charges - a fundamental problem in physics -. Prompted by this, Rob Corless and developers of the Maple computer algebra system realized that "the Lambert  $W$  function has been widely used in many fields, but because of differing notation and the absence of a standard name, awareness of the function was not as high as it should have been [12]."

*Note.* The general Lambert function is a multivalued function. Here, only the principal branch  $W_0$  is useful, the 0 indexing being omitted systematically.

*Note.* The principal branch of the Lambert function is a smooth monotonous strictly increasing function defined over  $\Re$  for  $x > -\frac{1}{e}$ .

*Note.* An approximate value of  $W(x)$  is also

$$W(x) = \text{Ln}x - \text{Ln}(\text{Ln}x) + o(1)$$

The later is not used in our own numerical evaluations as it is much too far off the required precision. Instead, we use systematically the "*lambertw(x)*" function provided within the Pari gp on-line application.

#### 4. DEFINING THE APPROPRIATE FRAME OF REFERENCE

**Proposition 1.** *The  $n_{th}$  solution of the set 2, thus verifying  $\text{Re}(\zeta(s)) = 0$  and  $\text{Im}(\zeta(s)) \neq 0$ , follows a smooth monotonous ordinates' evolution  $tr_n$  given by*

$$tr_n = La_{Re}(n) - (La_{Re}(n) - La_{Re}(n-1)) \cdot \epsilon_2(n) \quad (5)$$

where

$$La_{Re}(n) = 2\pi \frac{n - 11/8}{W(\frac{n-11/8}{e})} \quad (6)$$

and where, for  $n \geq 1$ , the maximum deviation is

$$0 < \epsilon_2(n) < \frac{1}{2000} n^{-1/2} \quad (7)$$

provided that the first element of the  $S2$ -set is indexed with  $n = 0$ .

**Proposition 2.** *The  $n_{th}$  solution of the set 3, thus verifying  $\text{Re}(\zeta(s)) \neq 0$  and  $\text{Im}(\zeta(s)) = 0$ , follows a smooth monotonous ordinates' evolution  $ti_n$  given by*

$$ti_n = La_{Im}(n) - (La_{Im}(n) - La_{Im}(n-1)) \cdot \epsilon_3(n) \quad (8)$$

where

$$La_{Im}(n) = 2\pi \frac{n - 7/8}{W(\frac{n-7/8}{e})} \quad (9)$$

and where, for  $n \geq 1$ , the maximum deviation is

$$0 < \epsilon_3(n) < \frac{1}{2000}n^{-1/2} \quad (10)$$

provided this time that the starting element of the  $S3$ -set is indexed with  $n = -1$ .

Graphic data are collected in figures 27 and 28.

*Note.* The difference between the two sets' parametrisation of  $a$  is  $-7/8 - (-11/8) = 1/2$ . The middle value is  $-11/8 + 1/4 = -9/8$ , which adding the index value 2 give back the approximate position of the first Riemann zero corresponding parameter  $a = 7/8$ .

**Proposition 3.** *Pairing of the sets 2 and 3: With the exception of  $n = -1$ , to each element of ordinate  $tr_n$  of the set 2 corresponds an element  $ti_n$  of the set 3, such that*

$$tr_n - ti_n = La_{Re}(n) - La_{Im}(n) - \epsilon_1(n) \quad (11)$$

where, for  $n > 1$ , the deviation is such that (see also figure 29)

$$0 < \epsilon_1(n) < \frac{1}{1000}n^{-3/2} \quad (12)$$

and where  $La_{Re}(n)$  and  $La_{Im}(n)$  are defined by the equations 6 and 9.

*Note.* The knowledge of the exact evolutions of  $\epsilon_1(n)$ ,  $\epsilon_2(n)$  and  $\epsilon_3(n)$  is not crucial. What is relevant is their respective convergence to 0 which is much faster than the narrowing of two successive elements of the sets 2 or 3.

This said, we ought to explain now why it is pertinent to call the previous frame an appropriate reference.

## 5. THE PAIRING OF CANCELLATIONS

Let us call partial cancellations the event where either  $Re(\zeta(s))$  or  $Im(\zeta(s))$  cancel on the critical line, the "or" being the exclusive or. Table 1 provides in strict increasing order a sample of those partial cancellations, as well as the complete cancellations corresponding to the non-trivial zeros of the Riemann function. Appendix B provides all of the examples  $s$  such that  $Im(s) < 100$ .

Except for the two first line of data, this table shows a pairing of the cancellations. For each non-trivial zero on the critical line, it happens that there is one partial cancellation event that we may associate. Appendix F provides the graphics of the pairings for the 50000+50000 first of them.

Let us call  $s = sz$  the coordinate of a non-trivial zero and  $s = sp$  its pairing companion. When the cases  $Re(\zeta(s)) = 0$  are examined, we get  $Im(\zeta(sp)).(Im(sp) - Im(sz)) > 0$ . The same kind of events holds for the cases  $Im(\zeta(s)) = 0$  but this time we get  $Re(\zeta(sp)).(Im(sp) - Im(sz)) > 0$ . Let us note that when  $Im(\zeta(s)) = 0$ , here and in the examples of the appendix, we observe that  $Im(sp) - Im(sz) > 0$  (because  $Re(\zeta(sp)) > 0$ ).

TABLE 1. Pairing of partial cancellations

| Set 2: $Re(\zeta(s)) = 0$ |                | Set 3: $Im(\zeta(s)) = 0$ |                |
|---------------------------|----------------|---------------------------|----------------|
| $Im(s)$                   | $Im(\zeta(s))$ | $Im(s)$                   | $Re(\zeta(s))$ |
|                           |                | 3.4362182                 | 0.5641510      |
| 0.8195453                 | -0.8255143     | 9.6669081                 | 1.5318207      |
| 14.1347251                | 0              | 14.1347251                | 0              |
| 14.5179196                | 0.3122704      | 17.8455995                | 2.3401817      |
| 20.6540450                | -0.4227757     | 21.0220396                | 0              |
| 21.0220396                | 0              | 23.1702827                | 1.4574270      |
| 25.0108576                | 0              | 25.0108576                | 0              |
| 25.4915082                | 0.6888099      | 27.6701822                | 2.8450912      |
| 29.7385103                | -0.9855390     | 30.4248761                | 0              |
| 30.4248761                | 0              | 31.7179800                | 0.9252646      |

This is however not a systematic result. The smallest two exceptions are  $Im(sp) = 282.4547208235 \dots$  for which  $Re(\zeta(sp)) = -0.0276294989 \dots$  and  $Im(sp) = 295.5839069742 \dots$  for which  $Re(\zeta(sp)) = -0.0169003909 \dots$

A note important notice here is that if we are looking for a set acting as the center of some distribution, because set 2 and set 3 are "equally" shifted, only one can fit and the candidate to favour is, from the first sample of values review, the set 2.

Let us then compare the set 1 and set 2 imaginary part  $t_n$  and  $tr_n$  advancing by decade in the index  $n$ . The results are given in table 2. The data for set 1 is obtained at reference [7]. In this table, we no more use

TABLE 2

| $n$       | Set1            | Set2            | $t_n - tr_n$ | $\frac{t_n - tr_n}{\left(\frac{2\pi}{Ln(n/2\pi)}\right)}$ |
|-----------|-----------------|-----------------|--------------|---|
| 1         | 14.134725       | 14.521347       | -0.38662     | -0.0499   |
| $10^3$    | 1419.42248      | 1419.51776      | -0.09528     | -0.0822   |
| $10^4$    | 9877.78265      | 9877.62962      | 0.15304      | 0.179   |
| $10^5$    | 74920.8275      | 74920.8910      | -0.06353     | -0.0949   |
| $10^6$    | 600269.6770     | 600269.6379     | 0.03906      | 0.0713  |
| $10^7$    | 4992381.0140    | 4992381.1105    | -0.09653     | -0.209  |
| $10^8$    | 42653549.7610   | 42653549.7735   | -0.01254     | -0.0314   |
| $10^9$    | 371870203.837   | 371870204.0508  | -0.21377     | -0.609  |
| $10^{10}$ | 3293531632.397  | 3293531632.259  | 0.1382       | 0.442   |
| $10^{11}$ | 29538618431.613 | 29538618431.813 | -0.2002      | -0.710  |

for  $n > 1000$  the value  $tr_n = Im(s)$  such that  $Re(\zeta(s)) = 0$ , but instead, because the two results are so close numerically, we opt for  $tr_n \approx La_{Re}(n) =$

$2\pi(n-11/8)W(\frac{n-11/8}{e})$ . This table shows at high index a remarkable matching between the two sets.

Using additional data available at reference [8], the largest height of ordinates we found readily on-line, we still get an excellent correspondence between the  $n^{th}$  Riemann's zero and the  $n^{th}$  element of set 2, as table 3 confirms. In this table,  $lag = 1.370919909931995300000 \cdot 10^{22}$ . The spacings  $t_n - tr_n$  are in general much closer than in table 2. The pairing is still fully effective.

TABLE 3

| $n - 10^{22}$ | Set1<br>$t_n - lag$ | Set2<br>$tr_n - lag$ | $t_n - tr_n$ | $\frac{t_n - tr_n}{(\frac{2\pi}{Ln(n/2\pi)})}$ |
|---------------|---------------------|----------------------|--------------|--|
| 9990          | 9566.96777          | 9566.94111           | 0.02665      | 0.199  |
| 9991          | 9567.07324          | 9567.07528           | -0.00203     | -0.015   |
| 9992          | 9567.20137          | 9567.20944           | -0.00807     | -0.06  |
| 9993          | 9567.30864          | 9567.3436            | -0.03497     | -0.261   |
| 9994          | 9567.45599          | 9567.47777           | -0.02178     | -0.162   |
| 9995          | 9567.67736          | 9567.61193           | 0.06543      | 0.488  |
| 9996          | 9567.82092          | 9567.7461            | 0.07483      | 0.558  |
| 9997          | 9567.8998           | 9567.88026           | 0.01954      | 0.146  |
| 9998          | 9568.09053          | 9568.01443           | 0.07611      | 0.567  |
| 9999          | 9568.15106          | 9568.14859           | 0.00247      | 0.018  |
| 10000         | 9568.33539          | 9568.28276           | 0.05263      | 0.392  |

*Note.* As the Riemann hypothesis is concerned, there is more than a mild signal issued by the pairing phenomena. Indeed, to which reference point on the critical line could be associated a non-trivial zero outside the critical line using the knowledge of such "random" abscissa?

## 6. GAUSSIAN DISTRIBUTIONS

Recall that the set 1 is defined by  $\{Re(\zeta(s)) = 0 \text{ and } Im(\zeta(s)) = 0\}$  and set 2 by  $\{Re(\zeta(s)) = 0 \text{ and } Im(\zeta(s)) \neq 0\}$  within the critical band.

**Proposition 4.** *Pairing of the sets 1 and 2: To each element of ordinate  $t_n$  of the set 1 correspond an element  $tr_n$  of the set 2. Moreover*

$$t_n - tr_n = G_r(n) \quad (13)$$

where, for  $n = i, n = i + 1, \dots, n = i + j, i \in N, j \in N$ , a sufficient large range of natural number  $n$ ,  $G_r(n)$  has a centred Gaussian distribution.

Figures 5 and 6 compares the distributions of a sample of 10000 values of  $\epsilon_2(n) = (tr_n - La_{Re}(n))/(La_{Re}(n) - La_{Re}(n - 1))$  classified by increasing values with a Gaussian distribution of same standard deviation. Before

getting to this comparison, which superposition is trivial, we checked the matching of the cumulative distribution function of the sample (for distribution's basic definitions refer to [14]) with the expected distribution type. The comparison of these cumulative distribution functions is shown in figure 4.

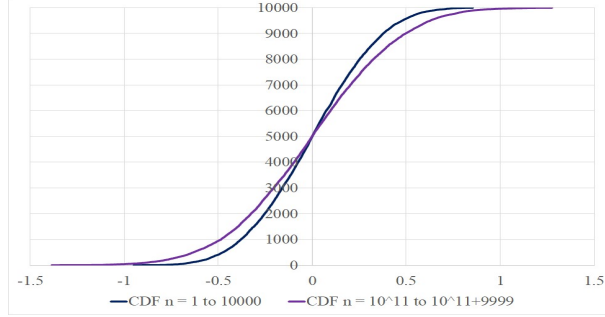


FIGURE 4.  
Cumulative distribution functions  
Samples 1 and 2

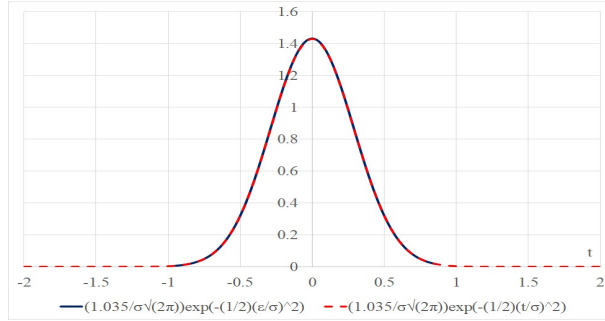


FIGURE 5. Sample 1 :  
Gaussian distribution  
 $n = 1$  to 10000

This means that the distribution  $G_r(n)$  of the locus of the set  $S1$  of Riemann zeros is centred when taking as reference the set 2. As Riemann zeros get closer one to each other, one might then expect some increasing repulsion effect from the centred values, therefore a Gaussian distribution with increasing standard deviations  $\sigma$ . Numerical verifications confirm effectively such expectation. The practical distribution samples, we choose here to verify numerically the proposition, are samples of 1000 successive results starting at index  $n$ .

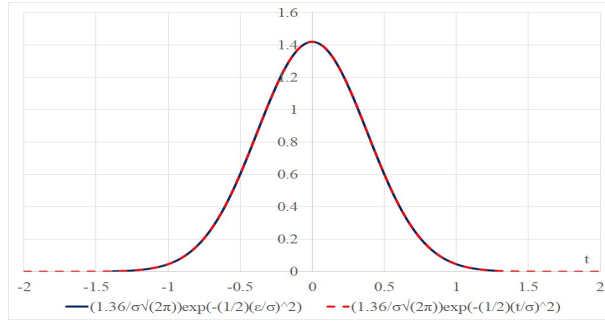


FIGURE 6. Sample 2 :  
Gaussian distribution  
 $n = 10^{11}$  to  $10^{11} + 9999$

A "wild" approximation of the standard deviation, as applied by table 11 and figure 32 (see appendix D), might be given by the formula

$$\sigma_{app}(n) = \frac{1}{8} + \frac{Ln(Ln(n + 500))}{4\pi} \quad (14)$$

Although using  $\pi$  and only natural numbers in the coefficients, which makes it look like an exact asymptotic formula, this approximation function so far is just a guess. Within  $Ln(Ln())$ , we use of course  $n+500$  because the sample contains 1000 elements. For higher values of  $n$ , it can be neglected but not for  $n < 10000$ . At much higher height of ordinates, with the help of the data provided at reference [8], we confirm the proximity to our assumption within the table 4.

TABLE 4

| $n$                               | $\sigma(n)$ | $\sigma_{app}(n)$ | $\Delta r(n)$ |
|-----------------------------------|-------------|-------------------|---------------|
| $10^{21} + 1$ to $10^{21} + 1000$ | 0.4340      | 0.4336            | -0.082 %      |
| $10^{22} + 1$ to $10^{22} + 1000$ | 0.4310      | 0.4373            | 1.467 %       |

This formula means a very slow increase of the standard deviation. We give in table 5, in addition to  $\sigma$ , the  $3\sigma$  values corresponding to the approximative probability 99.73% for the solutions to be present within  $tr_n$  plus or minus this range. We compare also, via a ratio, the  $6\sigma$  spacing with the average asymptotic distance between Riemann zeros (or elements of our reference frame) using the standard asymptotic  $2\pi/Ln(\frac{n}{2\pi})$  spacing.

When  $n$  tends towards infinity, although the absolute distance to the presume position of a Riemann zero may be small, its index compared with the index of the nearest point of the reference frame may be quite different in absolute value (but not in relative value). That doesn't mean at all that the pairing slowly vanishes. It means only that there can be some "wide"

TABLE 5

| $n$            | $\sigma$ | $3\sigma$ | $\frac{6\sigma}{2\pi/Ln(\frac{n}{2\pi})}$ |
|----------------|----------|-----------|---|
| $10^{100}$     | 0.558    | 1.674     | 122                                       |
| $10^{200}$     | 0.613    | 1.839     | 268                                       |
| $10^{300}$     | 0.645    | 1.936     | 425                                       |
| $10^{1000}$    | 0.752    | 2.257     | 1628                                      |
| $10^{10000}$   | 0.941    | 2.822     | 20322                                     |
| $10^{100000}$  | 1.129    | 3.387     | 243525                                    |
| $10^{1000000}$ | 1.317    | 3.952     | 2838159                                   |

late comers, then in-advance candidates, and in between a catching-up. This shifting is however a very rare scenario.

## 7. SHIFTING OF ORDINATES

Let us label an element of set 1 by " $-ri$ " and an element of set 2 by " $-re$ ". The most regular pairing pattern would be, ordering the ordinates of the sequences by increasing values, something like " $-ri - re - ri - re - ri - \dots$ ". Of course, this is impossible in a long sequence as we have seen that the distribution of the elements of set 1 is Gaussian compared with the position of the elements of set 2, therefore having as well later comers as in-advance candidates.

So let us have a look at consecutive " $-ri$ " elements. Let us start with two consecutive " $-ri - ri$ ". We count them as one event each. If we get three of them " $-ri - ri - ri$ ", we will count them as two events. If we get four of them " $-ri - ri - ri - ri$ ", we will count them as three events and so on. With the same samples of 1000 elements used to establish the standard deviation approximation  $\sigma_{app}$ , we collect the proportion of the consecutive pairs' pattern " $-ri - ri$ ". Having 2000 elements (adding 1000 " $-ri$ " and 1000 " $-re$ "), we may have at most 1000 consecutive " $-ri$ " (followed or preceded by 1000 consecutive " $-re$ "). So our proportions will be evaluated by dividing the number of consecutive pairs by 1000.

Here again a "wild" approximation of the proportions, as applied by table 12 and figure 33 (see appendix E), and labelled  $\kappa_{app}(n)$ , might be given by the formula

$$\kappa_{app}(n) = \frac{1}{5\sqrt{\pi}} + \frac{1}{4 Ln(Ln(n + 500))} \quad (15)$$

As figure 33 shows the collected data "behaviour" is much more bumpy and the interpretation driven here may be subject to some doubt. Additional data, with the same data help [8], still corroborates fairly the approximation as the reader can verify in table 6.

If the assumption is correct, the asymptotic proportion would be around  $\frac{1}{5\sqrt{\pi}} \approx 0.113$ , and the said proportion would be therefore almost constant in

TABLE 6

| $n$                               | $\kappa$ | $\kappa_{app}(n)$ | $\Delta r(n)$ |
|-----------------------------------|----------|-------------------|---------------|
| $10^{21} + 1$ to $10^{21} + 1000$ | 0.182    | 0.1773            | -2.59 %       |
| $10^{22} + 1$ to $10^{22} + 1000$ | 0.176    | 0.1765            | 0.30 %        |

a wide range as soon as  $n$  is large enough. This assumption is reflected in table 7.

TABLE 7

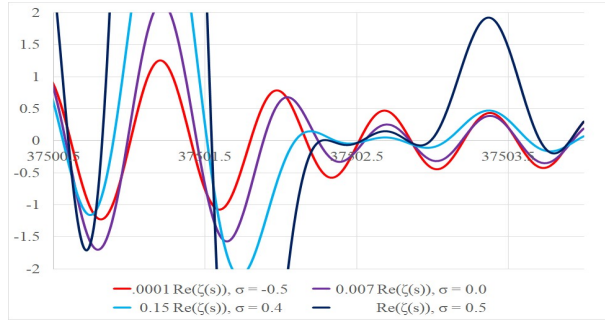
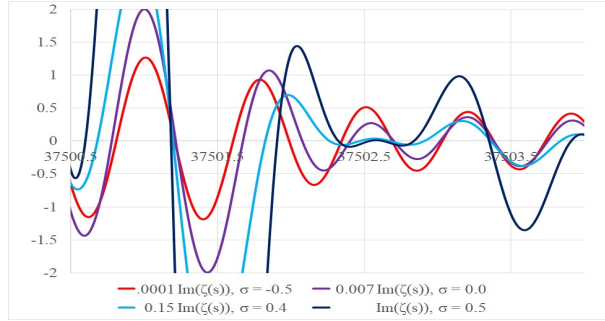
| $n$            | $\kappa_{app}(n)$ |
|----------------|-------------------|
| $10^{100}$     | 0.159             |
| $10^{200}$     | 0.154             |
| $10^{300}$     | 0.151             |
| $10^{1000}$    | 0.145             |
| $10^{10000}$   | 0.138             |
| $10^{100000}$  | 0.133             |
| $10^{1000000}$ | 0.130             |
| $\infty$       | $\approx 0.113$   |

The reader will note that 3 consecutive sequences ” $-ri - ri - ri-$ ” are rare events. There are only 3 happening among the first 50000 pairings, 20 in the  $n = 10^{21} + 1$  to  $10^{21} + 10000$  range and 15 in the  $n = 10^{22} + 1$  to  $10^{22} + 10000$  range. The detailed data is given in appendix F. To show that these events have a Gaussian trend (and why would they not ?) would require a huge calculation for no obvious crucial necessity.

## 8. SINUSOIDAL BIRTH OF CURVES

Recall that  $s = \sigma + i \cdot t$  using the standard coordinates settings and that here  $\sigma$  has no relationship with the standard deviation writing convention. Then let us compare the evolution of the curves  $Re(\zeta(s))$  within a small range of values of  $t$  as  $\sigma$  take values starting with some negative value (here  $-0.5$ ) up to  $1/2$  the center of the critical band. Let us compare also  $Im(\zeta(s))$  in the same way. These two cases are given in figures 7 and 8. The curves having very different amplitudes, we use scaling factors, as indicated in the figures’ legends, in order to make a more meaningful comparison.

The reader, having a close look at the case  $\sigma = -0.5$ , discovers an almost periodic amortized wave. The wave length diminishes smoothly towards an asymptotic trend (the expected  $2\pi/Ln(\frac{t}{2\pi})$  ratio). As  $\sigma$  increase towards  $1/2$ , the regularity of the patterns diminishes significantly. Let us observe that the shifts occur essentially within the critical band between  $\sigma = 0$  and  $1/2$ , that is the curves have not much ”time” to adjust to the ”disrupt

FIGURE 7. Trajectory  $Re(\zeta(s))$  versus  $t$ FIGURE 8. Trajectory  $Im(\zeta(s))$  versus  $t$ 

positions”, and therefore the Riemann zeros will stay in the vicinity of the ”ideal” positions.

*Note.* Starting with a sufficient negative value of  $\sigma$  and increasing this value, let us consider the intersections of the curves  $Re(\zeta(s))$  with the  $t - axis$ . We know, resulting from the pairing mentioned earlier, that half of the intersections will move to the positions of the set 1 and half to that of the set 2. Nevertheless, as the figure 7 shows (and equally for set 1 and set 3 in figure 8), the order of the positions of each intersection stays the same in the process. We emphasize that, starting with the early almost sinusoidal wave (ignoring the progressive change of the amplitude phenomena), the belonging of the intersections with the  $t - axis$  to such or such sets cannot be traced by keeping an eye on the evolution of a mere initial alternating ”yes – no – yes – no – ...” positioning. There is some property, certainly related to the prime numbers’ positions or spacings which determines from the start the belonging status to the final type of sets. Finding the related code to the prime numbers would allow even more to be knowledgeable in regard to the zeros’ locations.

We mentioned the necessity of a scaling factor to compare the curves. The following factor  $sc(\sigma, t)$  constitutes a good start for such enterprise and brings the curves within an approximative amplitude  $\pm 1$  when  $\sigma$  is kept

within the range  $[-50, -1]$ :

$$sc(\sigma, t) = \frac{5}{2} \left( t^{-\frac{1}{2} + (1 - \frac{1.83806}{\ln(t)}) \cdot \sigma} \right) \quad (16)$$

Of course, in the vicinity of the critical line  $\sigma = 1/2$ , most of the peaks' ordinates are much larger in absolute values than 1, but away down, like  $\sigma = -10$ , we get the typical case shown in figure 9. In this typical figure, over a moderate size interval of  $t$ , the curve is almost rigorously sinusoidal and this local interval can be taken larger and larger as  $t$  increases (while the wave length will shorten very slowly). This scaling factor is adapted as well for  $Re(\zeta(s))$  as for  $Im(\zeta(s))$ .

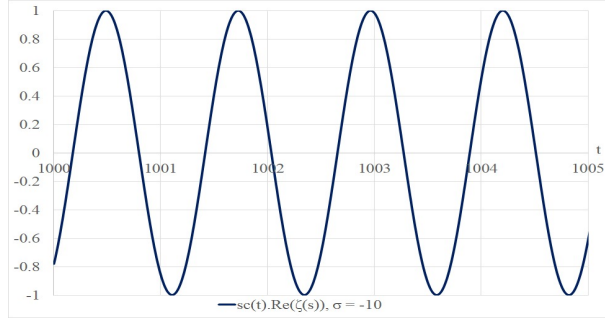


FIGURE 9. Trajectory  $sc(\sigma, t).Re(\zeta(s))$ ,  $\sigma = -10$

The proposed scaling factor fails badly for much larger negative values of  $\sigma$  than the mentioned domain, but not the almost sinusoidal property (ignoring the progressive change of the amplitude). The formula has to be revised. We don't give here such estimation as there is no use for larger values.

The origin of the sinusoidal trajectory is very simple to grasp with the following arguments. Indeed, one of the expression of the zeta function (valid over the entire complex plane except the unique point  $(1, 0)$ ), based on  $\sum_{n=0}^{\infty} f(s) = \frac{1}{2}f(0) + \int_0^{\infty} f(x)dx + i \int_0^{\infty} \frac{f(ix) - f(-ix)}{e^{2\pi x} - 1} dx$  [11], is the Abel-Plana type formula

$$\zeta(s) = \frac{1}{2} + \frac{1}{s-1} + 2 \int_0^{\infty} \frac{\sin(s \arctan x)}{(1+x^2)^{\frac{s}{2}} (e^{2\pi x} - 1)} dx.$$

Let us have  $s = \sigma + it$ ,  $\sigma$  a constant and  $t$  varying within a small range of values. Then  $\zeta(s) = \zeta(\sigma, t) = \zeta(t)$  and let us examine the expression under the integral  $\tau(t) = \sin((\sigma + it) \arctan x) (1+x^2)^{-\frac{1}{2}(\sigma+it)} (e^{2\pi x} - 1)^{-1}$ . Considering the terms dependant of  $t$ , we get  $\sin((\sigma + it) \arctan x) = \sin(\sigma.y) \cos(i.t.y) + \cos(\sigma.y) \sin(i.t.y) = \sin(\sigma.y) \cosh(t.y) + i \cos(\sigma.y) \sinh(t.y) \approx \exp(t.y) (\sin(\sigma.y) + i \cos(\sigma.y))$ , where  $y = \arctan x$  and  $\cosh(t.y) \approx \sinh(t.y) \approx \exp(t.y)$  for large enough  $t$  on one hand and  $(1+x^2)^{-\frac{1}{2}(\sigma+it)} = (1+x^2)^{-\frac{\sigma}{2}}$

$(\cos(t.Ln(\sqrt{1+x^2})) + i.\sin(t.Ln(\sqrt{1+x^2})))$  on the other hand. Multiplying all terms, we get  $\tau(t) \approx (e^{2\pi x} - 1)^{-1} (1+x^2)^{-\frac{\sigma}{2}} \exp(t.y) (\sin(\sigma.y) \cos(t.Ln(\sqrt{1+x^2})) - \cos(\sigma.y) \sin(t.Ln(\sqrt{1+x^2})) + i.(\cos(\sigma.y) \cos(t.Ln(\sqrt{1+x^2})) + \sin(\sigma.y) \sin(t.Ln(\sqrt{1+x^2})))) = (e^{2\pi x} - 1)^{-1} (1+x^2)^{-\frac{\sigma}{2}} \exp(t.y) (\sin(-t.Ln(\sqrt{1+x^2}) + \sigma.y) + i.\cos(t.Ln(\sqrt{1+x^2}) + \sigma.y))$ . So, disregarding the scaling correction applied by the exponential term  $\exp(y.t)$ , the expression under the integral  $\tau(t)$  is sinusoidal both for its real and imaginary parts. As the integration of a sine function is a cosine (and similarly a cosine gives a sine), we understand the origin to observed trajectory in figure 9. When  $\sigma$  is small in absolute value, of course, there is the perturbing effect of the additional terms  $\frac{1}{2} + \frac{1}{\sigma-1+it}$  to the integral of  $2\tau(t)$  to get back  $\zeta(t)$  as well as other tunings lost by the approximations.

### 9. THE IMAGINARY DOMAIN IS A STRONGHOLD

The consequence of the previous argument and of the regularly spaced positions of the partial cancellations is a fair realignment at each wave length between  $Re(\zeta(1/2 + it))$  and  $Re(\zeta(\sigma + it))$ ,  $\sigma < 1/2$ , as shows the example of figure 10.

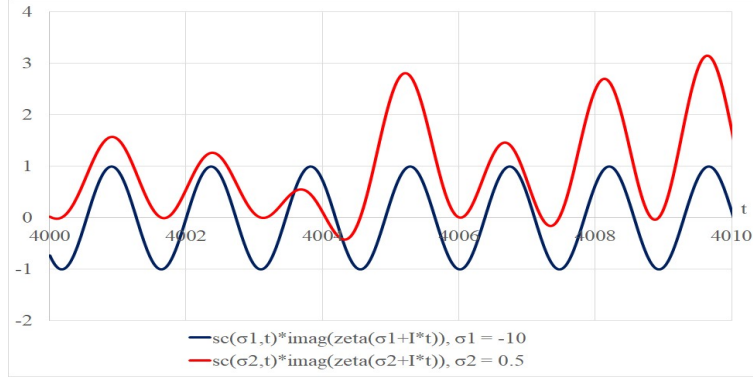


FIGURE 10.  
Trajectory  $sc(\sigma, t).Re(\zeta(s))$ ,  
 $\sigma = -10$  and  $\sigma = 1/2$

However, the topic is even more interesting when comparing the imaginary parts at each wave length (between  $Im(\zeta(1/2 + it))$  and  $Im(\zeta(\sigma + it))$ ,  $\sigma < 1/2$ ), as shows figure 11.

In this later case, the two curves stick to each other after each period when crossing the  $t$ -axis.

In an interval of  $t$  values, where there are three consecutive zeros' sequence " $-ri - ri - ri$ " within a wave length, there are some sharp adjustments necessary before and/or after the disrupting event, but the "sticking" still holds firmly. Figure 12 shows typically this kind of circumstances.

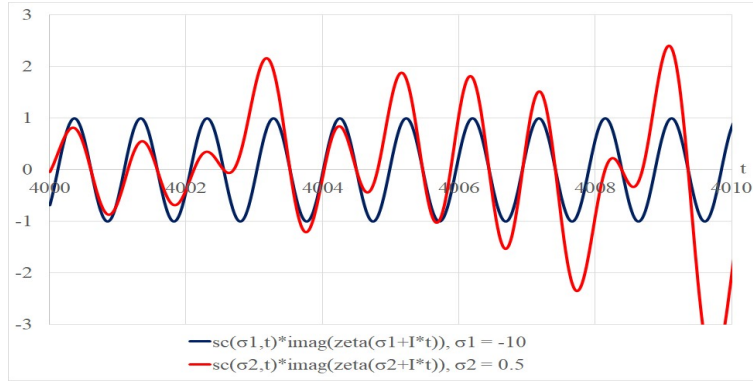


FIGURE 11.  
Trajectory  $sc(\sigma, t) \cdot Re(\zeta(s))$ ,  
 $\sigma = -10$  and  $\sigma = 1/2$

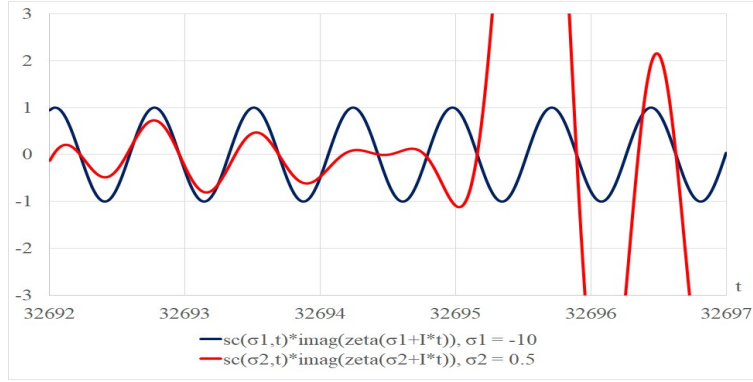


FIGURE 12.  
Trajectory  $sc(\sigma, t) \cdot Re(\zeta(s))$ ,  
 $\sigma = -10$  and  $\sigma = 1/2$

## 10. THE PARTIAL CANCELLATIONS' NETWORK

The sinusoidal feature, embedded in the Zeta function away from the critical band, allows the pairings of the partial and total cancellations sets. The existence of the pairings, by itself, is tempting for confirming the Riemann hypothesis as additional zeros outside the critical line would create necessarily havoc in these associations. In this section, we will take some distance from the critical line, to examine the network  $Re(\zeta(s)) = 0$  (or  $Im(\zeta(s)) = 0$ ) and its "well-behaviour" which any exception to the Riemann hypothesis would have certainly disturb a lot.

**10.1. Covering the left half critical band.** We will adopt in this section the convention  $s = \alpha + i\beta$  in order to construct another reference where  $s$  is

also expressed as a function of  $a$  and  $b$  and navigate between the two points of view.

In order to examine the entire  $0 < \alpha < 1/2$  domain, we consider the set of circles of radius  $1/4 + a$  and centre  $(1/4 - a, 0)$ , where  $a \in ]-1/4, \infty[$ . All of these circles are tangent to point  $(1/2, 0)$  on the left side, and continuously increasing  $a$ , one will cover the entire targeted area (and more).

The parametrized equation of each of these circles,  $a$  being fixed, is then given in complex representation by:

$$1/4 - a + (a + 1/4) \cdot (\cos(2\pi t) + i \cdot \sin(2\pi t))$$

where  $t$  describes a 1-length interval, for example:

$$-1/2 < t \leq 1/2$$

For  $t = 0$ , we get  $1/4 - a + (a + 1/4) \cdot (\cos(2\pi t) + i \cdot \sin(2\pi t)) = 1/2 + 0.i$ . For  $t = \pm 1/2$ , we get  $1/4 - a + (a + 1/4) \cdot (\cos(2\pi t) + i \cdot \sin(2\pi t)) = -2a + 0.i$ .

If we wish to reduce the points of the initial domain to  $0 < \alpha < 1/2$ , it suffices to restrict the previous domain of  $t$  to  $0 < 1/4 - a + (a + 1/4) \cdot \cos(2\pi t) < 1/2$ , that is

$$-a \cos((a - 1/4)/(a + 1/4))/2\pi < t < 0$$

to which we may add the symmetric with respect to the  $\alpha$ -axis. Doing so, we get for example the mapping from figure 13a to figure 13b (the left figure being a piece of a circle).

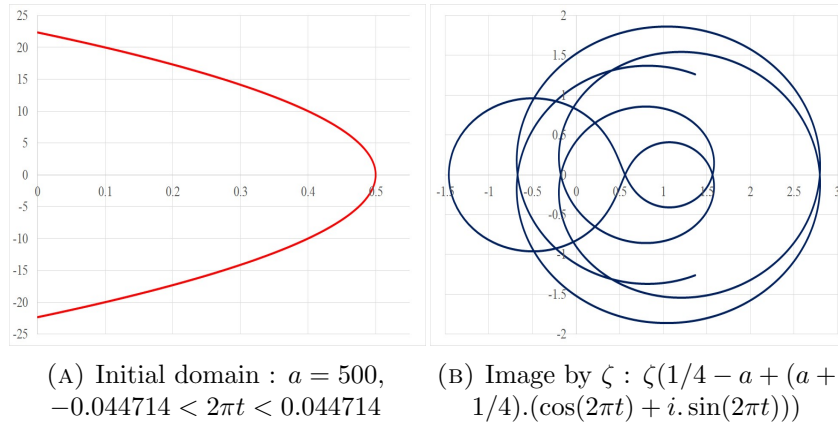


FIGURE 13

However, due to considerations appearing in the context of this article later on, it is quite more appropriate to take into account the whole domain  $-1/2 < t \leq 1/2$  (or  $0 \leq t \leq 1/2$ ) rather than the above restriction.

Hence, the domains of definition are an infinite set of circles inscribed in each other. In figure 14, we provide a sample where parameter  $a$  takes integer values between 0 and 8, the intermediate circles not being represented. The left half critical band is situated on the right side of that figure.

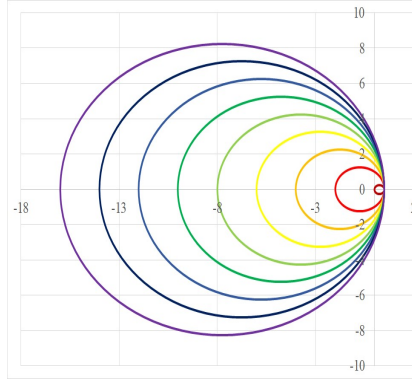


FIGURE 14.  
Domain of definition :  
 $a = 0$  to  $a = 8$ ,  $a \in \mathbb{N}$

One can then choose to navigate from one set of coordinates  $(a, t)$  to the other set  $(\alpha, \beta)$ :

$$\begin{aligned}\alpha &= 1/4 - a + (a + 1/4) \cdot \cos(2\pi t) \\ \beta &= (a + 1/4) \cdot \sin(2\pi t)\end{aligned}\tag{17}$$

or from the set of coordinates  $(\alpha, \beta)$  to the other set  $(a, t)$ , using the value of parameter  $a$  found in the first expression for the second one underneath:

$$\begin{aligned}a &= \frac{1}{2} \frac{(1/4 - \alpha)^2 + (\beta - 1/4)(\beta + 1/4)}{1/2 - \alpha} \\ t &= \frac{1}{2\pi} \arcsin\left(\frac{\beta}{a + 1/4}\right) = \frac{1}{2\pi} \arcsin\left(2\left(\frac{1}{2} - \alpha\right) \frac{\beta}{(1/2 - \alpha)^2 + \beta^2}\right)\end{aligned}\tag{18}$$

Note that if in this case  $\alpha = 1/2$  then  $a$  is undefined and  $t = 0$ .

**10.2. Axis intersections.** A typical example of the domains and codomains of the previously mentioned circles, choosing  $a = 12$ , gives the mapping from figure 15a to figure 15b.

The symmetry, in respect with the  $y = 0$  axis, of the initial circle, due to the functional equation, implies the symmetry of the image versus the same axis. Making the choice to take only positive values as an initial domain, the transformation from domain to codomain is as illustrated in figure 16a and figure 16b.

Let us consider then the codomain figures. We are going to collect some data on the set of intersections with the  $x = 0$  and  $y = 0$  axis.

**Proposition 5.** *The number of intersections  $\#I$  with the  $x$ -axis is equal to  $a$  over the domain  $0 \leq t < 1/2$ , for any value of  $a$  equal to a strictly positive integer. For  $a = 0$ , the number of intersections is equal to 1.*

$$\begin{aligned}\#I &= a & \text{if } a \in \mathbb{N}^* \\ \#I &= 1 & \text{if } a = 0\end{aligned}$$

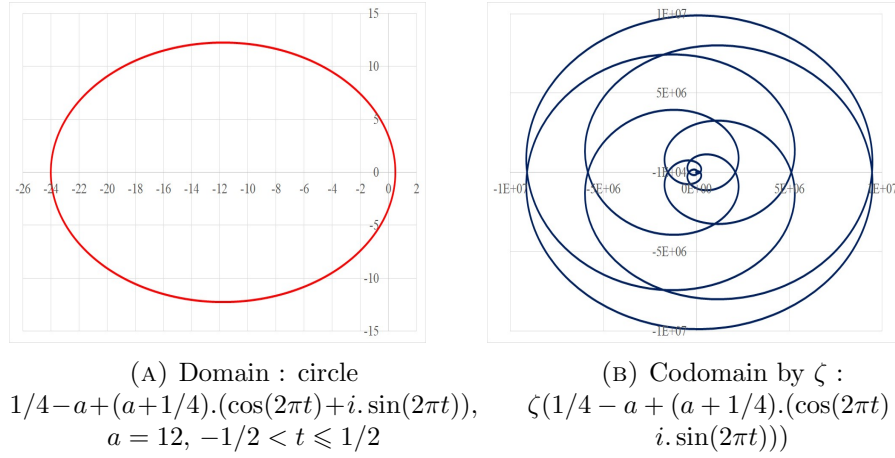


FIGURE 15

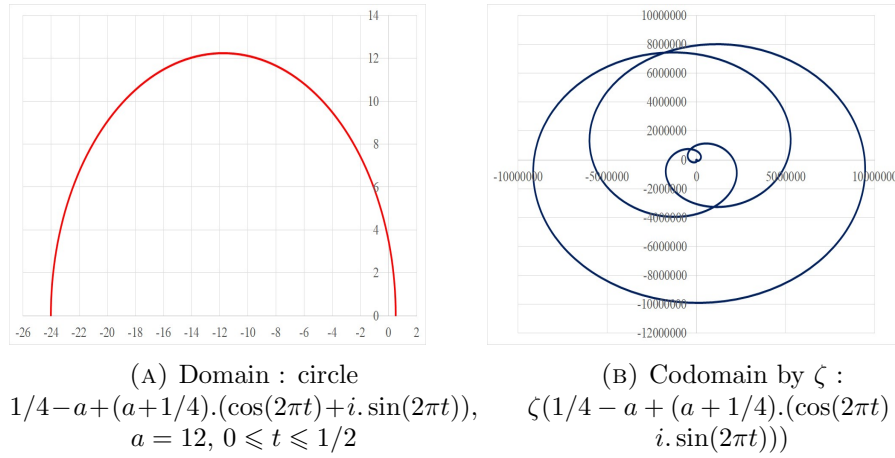


FIGURE 16

The underneath additional note is a direct consequence of the previous proposition. We provide it in order to make easier the reading (and checking) of the various graphics using sometimes  $-\pi < t \leq \pi$  and sometimes  $0 \leq t < \pi$  as domains of definition.

*Note.* The number of intersections, distinct or not,  $\#I_1$  with the  $x$ -axis is equal to  $2a$  over the domain  $-1/2 < t \leq 1/2$  for any value of  $a$  equal to a strictly positive integer. The number of distinct intersections  $\#I_2$  with the  $x$ -axis over the same domain is equal to  $a + 1$  for any value of  $a$  equal to a strictly positive integer.

$$\#I_1 = 2a, \#I_2 = a + 1, a \in \mathbb{N}^*$$

Besides for  $a = 0$ , we get

$$\#I_1 = 2 \text{ and } \#I_2 = 2$$

**Proposition 6.** *The intersections with the  $y$ -axis are all distinct. The number of intersections  $\#I$  with the  $y$ -axis is equal to  $a$  over the domain  $0 \leq t \leq 1/2$  for any value of  $a = n + \epsilon$ , where  $n \in N$  and  $0 < \epsilon < 1$ ,  $N$  the natural numbers including 0.*

$$\#I = n \setminus a = n + \epsilon, \quad 0 < \epsilon < 1$$

*Note.* If  $a \in N$ , there are a few cases  $a < 3$  to distinguish from the general result:

$$\#I = 0 \quad \text{if} \quad a = 0$$

$$\#I = 2 \quad \text{if} \quad a = 1$$

$$\#I = 3 \quad \text{if} \quad a = 2$$

$$\#I = a \quad \text{if} \quad a \in N \cap a \geq 3$$

*Note.* The number of intersections (all distinct)  $\#I_1$  with the  $y$ -axis is equal to  $2n$  over the domain  $-1/2 < t \leq 1/2$  for any value of  $a = n + \epsilon$ , where  $n \in N$  and  $0 < \epsilon < 1$ . The number of intersections  $\#I_2$  with the  $y$ -axis over the same domain is equal to  $2a - 1$  for any value of  $a$  equal to a strictly positive integer except for  $a = 0$  ( $\#I_2 = 0$ ) and  $a = 1$  ( $\#I_2 = 3$ ).

$$\#I_1 = 2n \quad \text{if} \quad a = n + \epsilon, \quad 0 < \epsilon < 1$$

$$\#I_2 = 0 \quad \text{if} \quad a = 0$$

$$\#I_2 = 3 \quad \text{if} \quad a = 1$$

$$\#I_2 = 2a - 1 \quad \text{if} \quad a \in N - \{0, 1\}$$

**Proposition 7.** *The value of the mantissa of  $a$ , for which an increase of the number of intersections  $\#I$  with the  $x$ -axis occurs, is strictly increasing and bounded by 1 excluded when  $a$  tends towards infinity.*

$$\text{mantissa}(a) = a - \lfloor a \rfloor \rightarrow 1^-, \quad a \rightarrow +\infty, \quad \#I \rightarrow \#I + 1$$

**Proposition 8.** *The approximate interpolation of the value of the mantissa, linked to the intersections' cardinal  $\#I$  increase, is given by:*

$$\text{mantissa}(a) = 1 - 0.615(a + 0.5)^{-0.33} \quad (19)$$

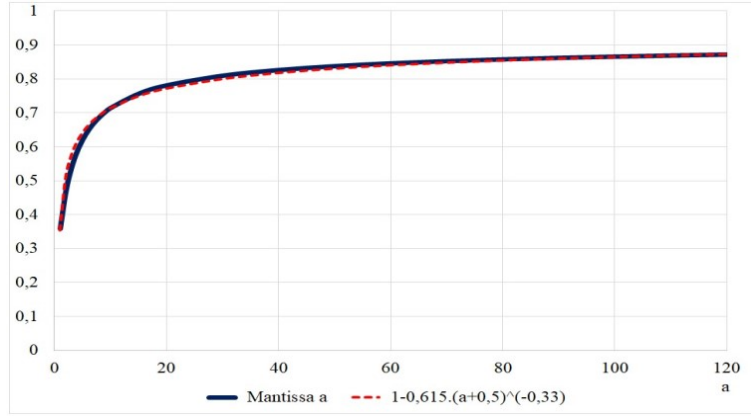
*The corresponding data are given in table 8 and figure 17.*

*Note.* To be precise, the depiction of the mantissa is not a continuous function as it takes actual values only when the number of intersections  $\#I$  with the  $x$ -axis increases.

*Note.* The presence of a non-trivial zero would cause havoc to a rule of thumb for the number of intersections and to the previous mantissa formula's smooth match.

TABLE 8. Mantissa values

| $n$ | $a$       | $mantissa$ | $approx$ | $n$ | $a$        | $mantissa$ | $approx$ |
|-----|-----------|------------|----------|-----|------------|------------|----------|
| 1   | 1.358632  | 0.358632   | 0.353276 | 20  | 20.780205  | 0.780205   | 0.772207 |
| 2   | 2.468381  | 0.468381   | 0.508165 | 30  | 30.808699  | 0.808699   | 0.800493 |
| 3   | 3.537299  | 0.537299   | 0.573760 | 40  | 40.825408  | 0.825408   | 0.818434 |
| 4   | 4.585247  | 0.585247   | 0.613479 | 50  | 50.836720  | 0.836720   | 0.831246 |
| 5   | 5.620606  | 0.620606   | 0.641244 | 60  | 60.845044  | 0.845044   | 0.841050 |
| 6   | 6.647788  | 0.647788   | 0.662248 | 70  | 70.851511  | 0.851511   | 0.848896 |
| 7   | 7.669365  | 0.669365   | 0.678955 | 80  | 80.856731  | 0.856731   | 0.855384 |
| 8   | 8.686942  | 0.686942   | 0.692712 | 90  | 90.861066  | 0.861066   | 0.860876 |
| 9   | 9.701567  | 0.701567   | 0.704334 | 100 | 100.864746 | 0.864746   | 0.865614 |
| 10  | 10.713951 | 0.713951   | 0.714345 | 110 | 110.867923 | 0.867923   | 0.869762 |
| 15  | 15.755717 | 0.755717   | 0.749768 | 120 | 120.870705 | 0.870705   | 0.873438 |

FIGURE 17. Mantissa of  $a$  matching an increase of the number of intersections  $\#I$ .

**Proposition 9.** *Similarly, but in a much simpler way as for the  $x$ -axis, the number of intersections  $\#I$  with the  $y$ -axis increases with the value of  $a$  each time parameter  $a$  reaches an integer value, that is each time the mantissa of  $a$  cancels:*

$$mantissa(a) = 0 \quad (20)$$

*Note.* The triviality of the mantissa of  $a$ , guiding the increase of the number of intersections with the  $y$ -axis, is a mirror indicator of some expected "triviality" of the mantissa  $a$  relative to the  $x$ -axis, this latter triviality being the smooth evolution shown in figure 17. Therefore, we get again a reminder that non-trivial zeros outside  $s = 1/2$  are not relevant.

In the rest of this article, we will focus on the  $x$ -axis intersections. Let us however note the existence of the same kind of pattern for the  $y$ -axis intersections.

TABLE 9. Sample of values  $u = 2\pi t(a)$ 

| $a$  | 1     | 2           | 3           | 4           | 5           | 6           | 7           | 8           | 9           |
|------|-------|-------------|-------------|-------------|-------------|-------------|-------------|-------------|-------------|
| $S0$ | 0     | 0           | 0           | 0           | 0           | 0           | 0           | 0           | 0           |
| $S1$ | $\pi$ | $0.4567\pi$ | $0.3064\pi$ | $0.2350\pi$ | $0.1916\pi$ | $0.1621\pi$ | $0.1407\pi$ | $0.1244\pi$ | $0.1115\pi$ |
| $S2$ |       | $\pi$       | $0.7124\pi$ | $0.5769\pi$ | $0.5117\pi$ | $0.4749\pi$ | $0.4545\pi$ | $0.4454\pi$ | $0.4449\pi$ |
| $S3$ |       |             | $\pi$       | $0.8202\pi$ | $0.7033\pi$ | $0.6446\pi$ | $0.6099\pi$ | $0.5886\pi$ | $0.5757\pi$ |
| $S4$ |       |             |             | $\pi$       | $0.8766\pi$ | $0.7751\pi$ | $0.7208\pi$ | $0.6865\pi$ | $0.6637\pi$ |
| $S5$ |       |             |             |             | $\pi$       | $0.9096\pi$ | $0.8216\pi$ | $0.7713\pi$ | $0.7380\pi$ |
| $S6$ |       |             |             |             |             | $\pi$       | $0.9306\pi$ | $0.8538\pi$ | $0.8074\pi$ |
| $S7$ |       |             |             |             |             |             | $\pi$       | $0.9446\pi$ | $0.8773\pi$ |
| $S8$ |       |             |             |             |             |             |             | $\pi$       | $0.9545\pi$ |
| $S9$ |       |             |             |             |             |             |             |             | $\pi$       |

 TABLE 10. Sample of values  $u = 2\pi t(a)$ 

| $a$  | 6           | 6.2         | 6.4         | 6.6         | 6.647788    | 6.8         | 7           |
|------|-------------|-------------|-------------|-------------|-------------|-------------|-------------|
| $S0$ | 0           | 0           | 0           | 0           | 0           | 0           | 0           |
| $S1$ | $0.1621\pi$ | $0.1573\pi$ | $0.1528\pi$ | $0.1485\pi$ | $0.1476\pi$ | $0.1445\pi$ | $0.1407\pi$ |
| $S2$ | $0.4749\pi$ | $0.4697\pi$ | $0.4651\pi$ | $0.4610\pi$ | $0.4602\pi$ | $0.4575\pi$ | $0.4545\pi$ |
| $S3$ | $0.6446\pi$ | $0.6363\pi$ | $0.6287\pi$ | $0.6218\pi$ | $0.6203\pi$ | $0.6156\pi$ | $0.6099\pi$ |
| $S4$ | $0.7751\pi$ | $0.7619\pi$ | $0.7501\pi$ | $0.7393\pi$ | $0.7369\pi$ | $0.7296\pi$ | $0.7208\pi$ |
| $S5$ | $0.9096\pi$ | $0.8864\pi$ | $0.8669\pi$ | $0.8499\pi$ | $0.8461\pi$ | $0.8349\pi$ | $0.8216\pi$ |
| $S6$ | $\pi$       | $\pi$       | $\pi$       | $\pi$       | $\pi$       | $0.9556\pi$ | $0.9306\pi$ |
| $S7$ |             |             |             |             | $\pi$       | $\pi$       | $\pi$       |

**Proposition 10.** *Let us have the explicit function of two variables  $\zeta(a, t) = \zeta(1/4 - a + (a + 1/4) \cdot (\cos(2\pi t) + i \cdot \sin(2\pi t)))$ . We consider the implicit application  $t(a)$  such as  $\text{Im}(\zeta(a, t)) = 0$ . It defines a network of continuous values  $t$  of the variable  $a$  with an additional curve for each incrementation of  $\#I$ ,  $\#I$  being the term defined in proposition 5.*

The data  $t(a)$ , for a sample of integer values of  $a$ , are given in table 9. Each line corresponds to an additional curve.

Following the curves' trajectories imposed by keeping  $\text{Im}(\zeta(1/4 - a + (a + 1/4) \cdot (\cos(2\pi t) + i \cdot \sin(2\pi t)))) = 0$ , we get the intermediary values of table 10 for  $a$  between 6 and 7, the reader will note the beginning of a new junction for the mantissa approximative value 6.647788 (as previously mentioned in table 8). The ordinate  $t = 1/2$  (written twice therefore) splits here into two values as the abscissa  $a$  increases.

The corresponding graphic representation is given by figure 18.

These are the curves which prolongation is linked to the trivial zeros of the Zeta function. One can observe a void between the first of the curve (excluding  $S0$  the trivial  $t = 0$  line) and the other ones. The reason of this empty space is that it's not the full picture which one is given in figure

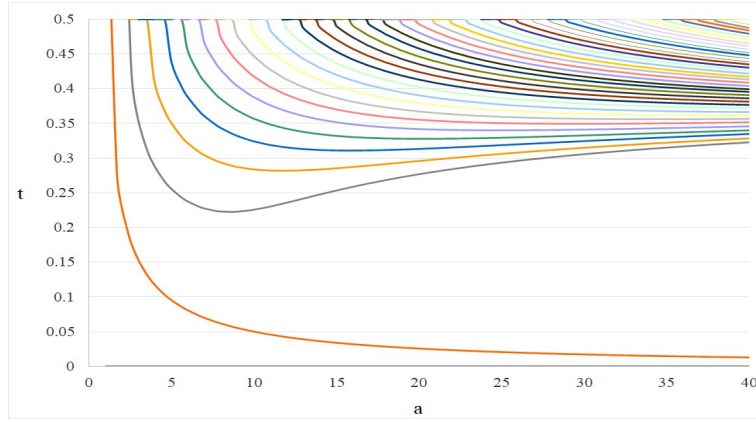


FIGURE 18. Network of curves  $t(a)$  such that  $\text{Im}(\zeta(1/4 - a + (a + 1/4) \cdot (\cos(2\pi t) + i \cdot \sin(2\pi t)))) = 0$

19. There, we have been completing it by the curves aiming at the non-trivial zeros and the partial zeros, something one could check with a careful tracking.

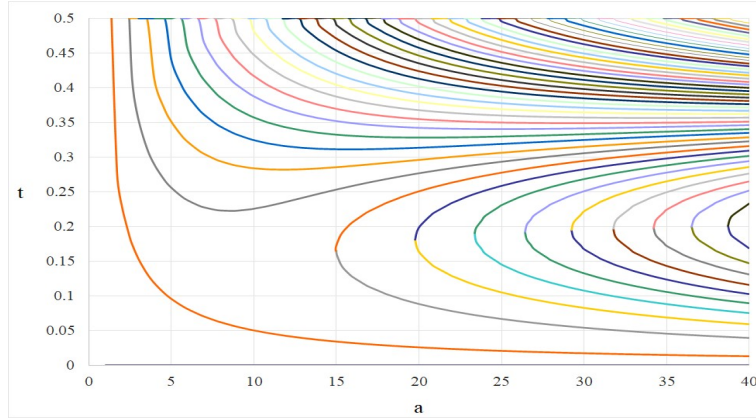


FIGURE 19. Network of curves  $t(a)$  such that  $\text{Im}(\zeta(1/4 - a + (a + 1/4) \cdot (\cos(2\pi t) + i \cdot \sin(2\pi t)))) = 0$

*Note.* The Zeta function is a smooth expression. With Occam's razor principle, it is difficult to imagine, in the initial  $\sum \frac{1}{n^s}$ , what would change the regular evolution of the network of curves shown in figure 19 on its way to infinity ( $a$  increasing). Of course, any non-trivial zero, outside  $\text{Re}(s) = 1/2$ , would create quite some havoc in this pattern.

*Note.* One can also represent the network of curves  $\text{Im}(\zeta(1/4 - a + (a + 1/4) \cdot (\cos(2\pi t) + i \cdot \sin(2\pi t)))) = 0$  within the system of coordinates  $(\alpha, \beta)$  where  $\alpha$  and  $\beta$  is defined by the equations labelled (17). The corresponding

network is shown in figure 20. This representation is however less appealing as the two patterns intermingle with confusing intersections while figure 19 allows to avoid that kind of phenomena. The diagonal pattern corresponds to the curves heading to the trivial zeros, the "partially horizontal" pattern heading towards the non-trivial zeros and their pairings in an totally ordered manner. One can trace the link from one figure to the another by the corresponding colors of the curves.

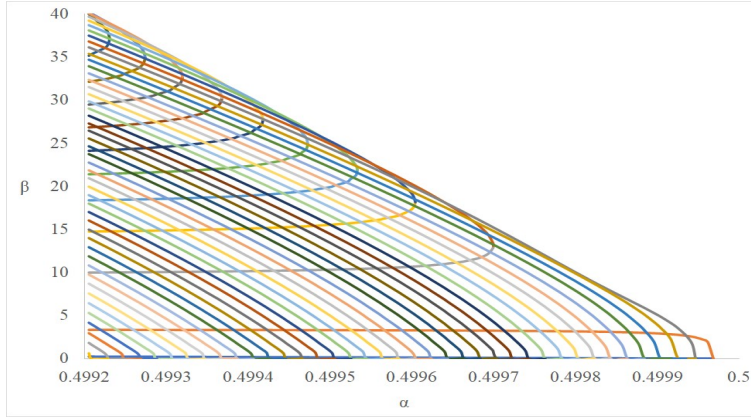


FIGURE 20. Network of curves  $(\alpha, \beta)$  such that  $Im(\zeta(1/4 - a + (a + 1/4) \cdot (\cos(2\pi t) + i \cdot \sin(2\pi t)))) = 0$

## 11. CONCLUSION

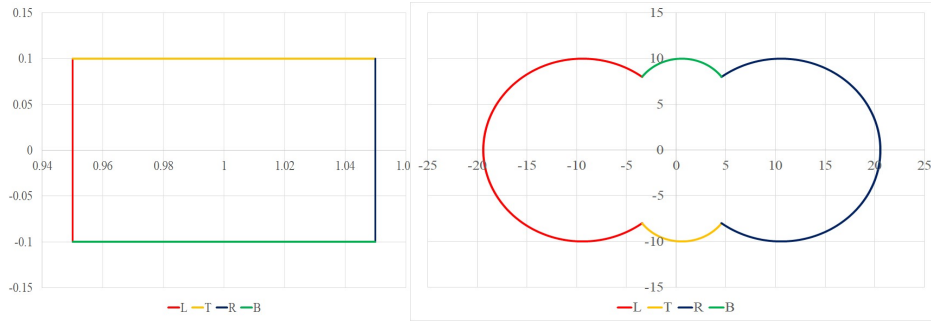
As presumed, there are a lot of quite simple features in the real and imaginary parts of the Zeta function:

- the real parts are constant;
- the imaginary parts of the solutions to partial cancellations lie on a smooth slowly contracting sinusoidal wave;
- there are the "same" number of solutions to partial cancellations  $Re(\zeta(s)) = 0$  as to total cancellations  $\zeta(s) = 0$ ;
- there are the "same" number of solutions to partial cancellations  $Im(\zeta(s)) = 0$  as to total cancellations  $\zeta(s) = 0$ ;
- the imaginary parts' distribution of the zeros of the Zeta function is Gaussian when referred to the adequate frame of reference, which is the set of cancellations  $Re(\zeta(s)) = 0$ , a reference that besides can be swapped asymptotically (in fact much earlier) for a simpler set related to Lambert function principal branch;
- the network of solutions  $s$  to  $Re(\zeta(s)) = 0$  (and  $Im(\zeta(s)) = 0$  likely) is as "well-tempered" as a Johann Sebastian Bach composition.

## APPENDIX A. CONFORMAL MAPS

The case around the pole (see figure 21) could have been an exception to the general rule as the value of the image diverges in the center. But adding the correspondence  $(1, 0) \rightarrow \infty$  preserves the bijection. When oriented,

FIGURE 21.  
Initial rectangle  $r$  delimiting  
 $\sigma = [0.95, 1.05]$ ,  $t = [-0.1, 0.1]$   
Image "rectangle"  $\zeta(r)$



the trajectory around the pole of the image is reversed compared to the trajectory of the initial rectangle.

Around the trivial zeros (see figures 22 and 23), there is no special phenomena.

FIGURE 22.  
Initial rectangle  $r$  delimiting  
 $\sigma = [-2.05, -1.95]$ ,  $t = [-0.1, 0.1]$   
Image "rectangle"  $\zeta(r)$

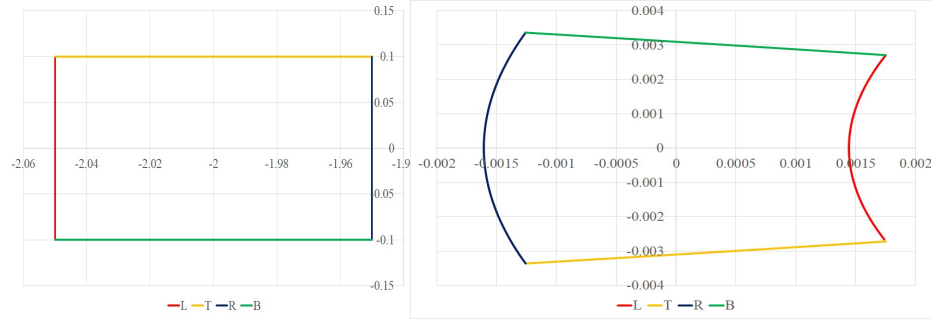
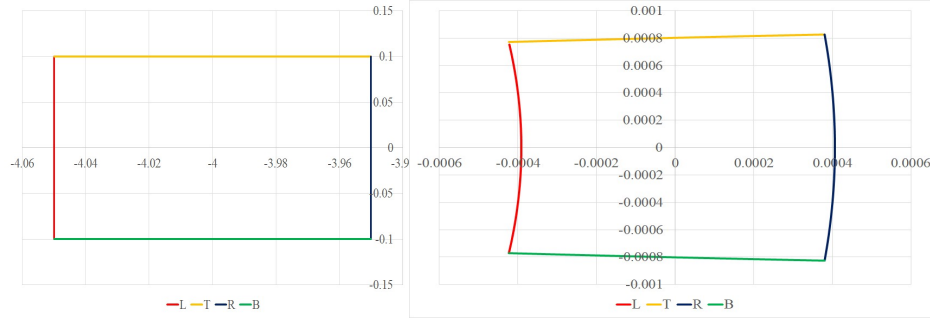
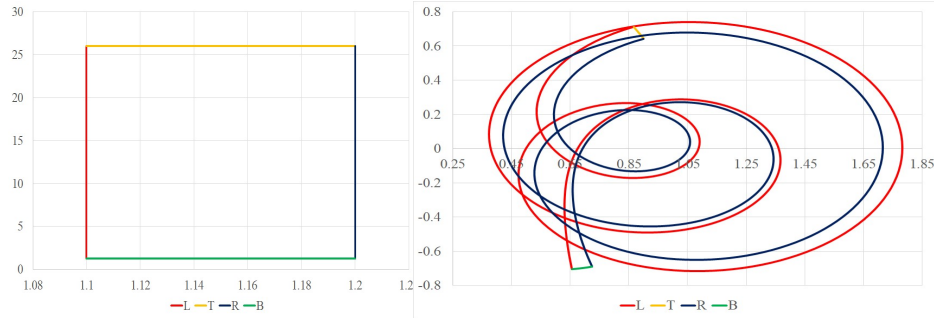


FIGURE 23.  
Initial rectangle  $r$  delimiting  
 $\sigma = [-4.05, -3.95]$ ,  $t = [-0.1, 0.1]$   
Image "rectangle"  $\zeta(r)$



For a typical case (see figure 24), over a broader interval, including zeros, the surfaces overlap and like Riemann surfaces would unfold and spiral around some middle axis in a 3D representation. It seems that except for the

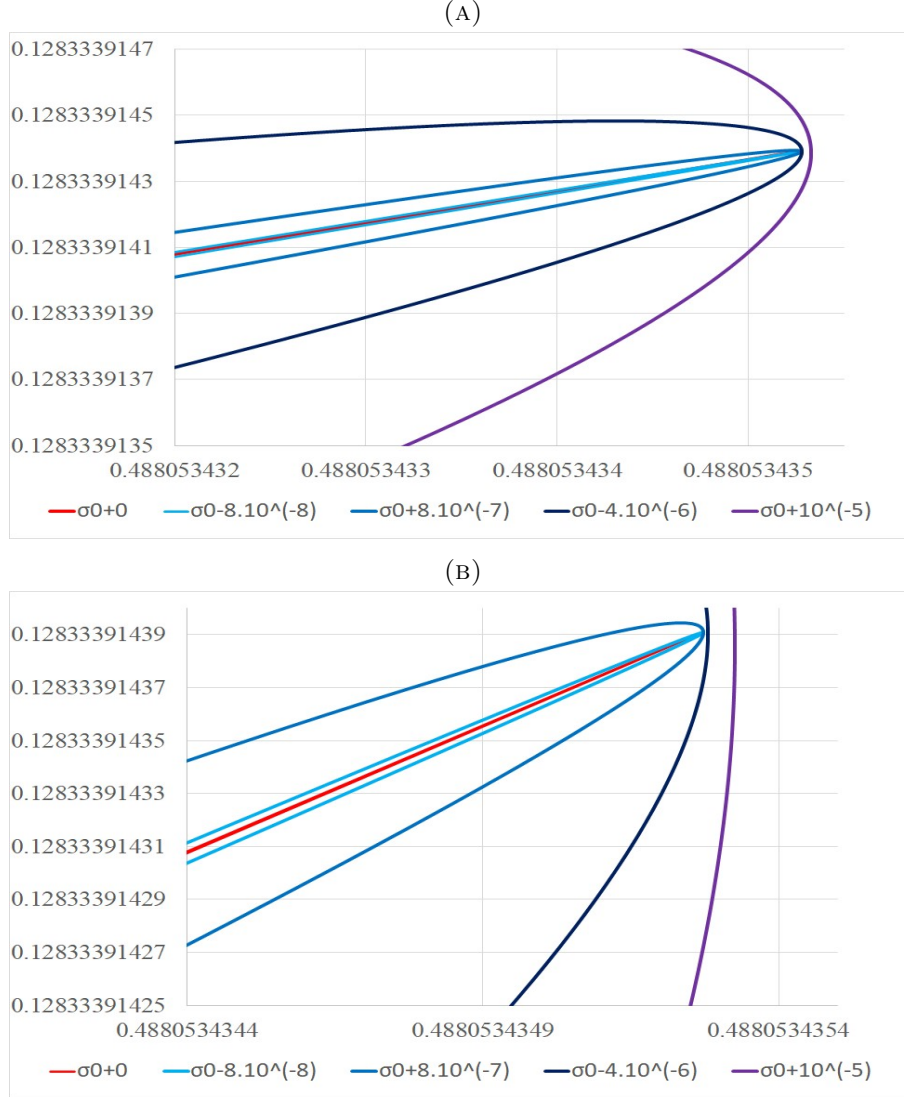
FIGURE 24.  
Initial rectangle  $r$  delimiting  
 $\sigma = [1.1, 1.2]$ ,  $t = [1.25, 26]$   
Image "rectangle"  $\zeta(r)$



pole's contour, all the other contours are oriented like the initial rectangle.

The event where  $\zeta'(s_0) = \zeta'(\sigma_0 + i.t_0) = 0$  appears as a limit case of the general feature. The curve  $\zeta(\sigma_0 + i.t)$ ,  $t \approx t_0$  is almost a straight line inwards and a straight line outwards (red curve). The surrounding curves are at arbitrary close distances but without ever meeting the limit curve. There is no crossing locally, every curve staying on its respective side of the other. Figure 25 *a* (and its close-up *b*) is a typical case. Here the derivative cancels for  $s_0 \approx 0.84873532 + i.60.14084577857$ . In this example, we alternate the sign of  $\Delta\sigma$  while we took increasing absolute values. At very large close-up, a rectangular domain will still give an almost rectangular image.

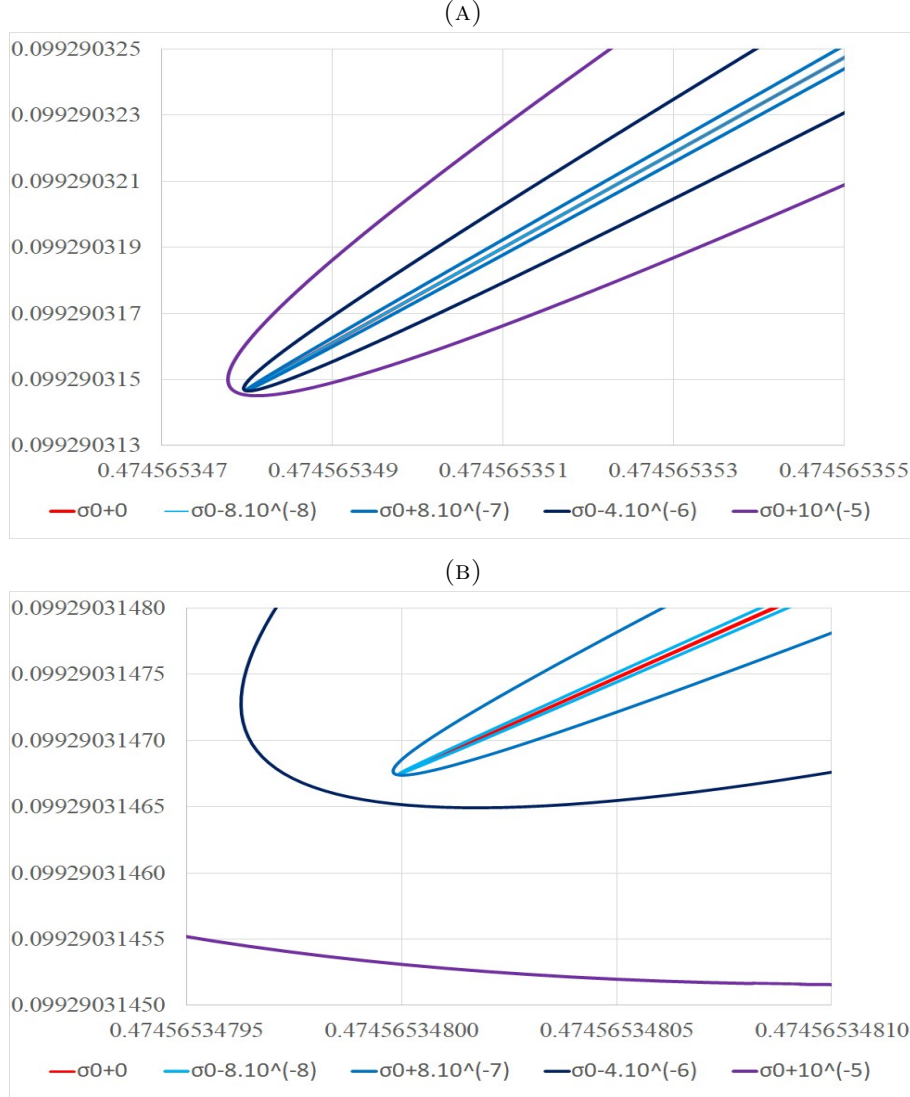
FIGURE 25.  
 $\sigma_0 = 0.84873532$   $t = [60.140715, 60.140967]$   
 Image  $\zeta(\sigma_0 + \Delta\sigma + t)$



In the case of second derivative's cancelling, it is this time the first derivative of  $\zeta$  that shows the previous pattern. Figure 26 *a* (and its close-up *b*) is a typical case. Here the second derivative cancels for  $s_0 \approx 0.9691707 + i.295.16838$ .

For a curious reader, a relevant remark may be: how to explain the simultaneous property of the  $\zeta$ -function being infinitely derivable and showing

FIGURE 26.  
 $\sigma_0 = 0.9691707$   $t = [295.16825, 295.1685]$   
 Image  $\zeta'(\sigma_0 + \Delta\sigma + t)$



in the same time straight lines coming in and going out within the former graphics? What happens in the vicinity of  $\sigma_0 + i.t_0$ ? The answer is a size-diminishing node (crunode), barely visible even at high magnification, therefore avoiding a cusp, and allowing any derivative's value and a smooth continuation through the non-singular point  $\sigma_0 + i.t_0$ .

## APPENDIX B. PARTIAL ZETA ZEROS

$$\alpha = \operatorname{Re}(s) = 0.5$$

| $\operatorname{Re}(\zeta(s)) = 0$ |                               | $\operatorname{Im}(\zeta(s)) = 0$ |                               |
|-----------------------------------|-------------------------------|-----------------------------------|-------------------------------|
| $\operatorname{Im}(s)$            | $\operatorname{Im}(\zeta(s))$ | $\operatorname{Im}(s)$            | $\operatorname{Re}(\zeta(s))$ |
|                                   |                               | 3.4362182                         | 0.5641510                     |
| 0.8195453                         | -0.8255143                    | 9.6669081                         | 1.5318207                     |
| 14.1347251                        | 0                             | 14.1347251                        | 0                             |
| 14.5179196                        | 0.3122704                     | 17.8455995                        | 2.3401817                     |
| 20.6540450                        | -0.4227757                    | 21.0220396                        | 0                             |
| 21.0220396                        | 0                             | 23.1702827                        | 1.4574270                     |
| 25.0108576                        | 0                             | 25.0108576                        | 0                             |
| 25.4915082                        | 0.6888099                     | 27.6701822                        | 2.8450912                     |
| 29.7385103                        | -0.9855390                    | 30.4248761                        | 0                             |
| 30.4248761                        | 0                             | 31.7179800                        | 0.9252646                     |
| 32.9350616                        | 0                             | 32.9350616                        | 0                             |
| 33.6237931                        | 1.0716783                     | 35.4671843                        | 2.9381215                     |
| 37.2567418                        | -0.6505448                    | 37.5861782                        | 0                             |
| 37.5861782                        | 0                             | 38.9992100                        | 1.7867218                     |
| 40.7000036                        | -0.3314003                    | 40.9187190                        | 0                             |
| 40.9187190                        | 0                             | 42.3635504                        | 1.0987569                     |
| 43.3270733                        | 0                             | 43.3270733                        | 0                             |
| 43.9935273                        | 1.3843203                     | 45.5930290                        | 3.6629029                     |
| 47.1646902                        | -1.6474277                    | 48.0051509                        | 0                             |
| 48.0051509                        | 0                             | 48.7107766                        | 0.6882924                     |
| 49.7738325                        | 0                             | 49.7738325                        | 0                             |
| 50.2332544                        | 0.7168152                     | 51.7338428                        | 2.0112139                     |
| 52.9703215                        | 0                             | 52.9703215                        | 0                             |
| 53.2140564                        | 0.5998411                     | 54.6752374                        | 2.9123905                     |
| 56.1185828                        | -0.7940224                    | 56.4462477                        | 0                             |
| 56.4462477                        | 0                             | 57.5451652                        | 1.7581649                     |
| 58.9559503                        | -0.5974902                    | 59.3470440                        | 0                             |
| 59.3470440                        | 0                             | 60.3518120                        | 0.5385858                     |
| 60.8317785                        | 0                             | 60.8317785                        | 0                             |
| 61.7335435                        | 2.0558319                     | 63.1018680                        | 4.1643988                     |
| 64.4574470                        | -1.7414112                    | 65.1125440                        | 0                             |
| 65.1125440                        | 0                             | 65.8008876                        | 1.0538773                     |
| 67.0798105                        | 0                             | 67.0798105                        | 0                             |
| 67.1327484                        | 0.0948357                     | 68.4535449                        | 1.5400583                     |
| 69.5464017                        | 0                             | 69.5464017                        | 0                             |
| 69.7637543                        | 0.4793063                     | 71.0638190                        | 1.9527373                     |
| 72.0671577                        | 0                             | 72.0671577                        | 0                             |
| 72.3541506                        | 0.8790431                     | 73.6351323                        | 3.6143950                     |
| 74.9071220                        | -1.8642143                    | 75.7046907                        | 0                             |
| 75.7046907                        | 0                             | 76.1704546                        | 0.5654782                     |
| 77.1448401                        | 0                             | 77.1448401                        | 0                             |
| 77.4254438                        | 0.4310013                     | 78.6723840                        | 1.2271237                     |
| 79.3373750                        | 0                             | 79.3373750                        | 0                             |
| 79.9115523                        | 1.7004816                     | 81.1432094                        | 3.9981977                     |
| 82.3676012                        | -1.6134986                    | 82.9103809                        | 0                             |
| 82.9103809                        | 0                             | 83.5849601                        | 1.1700214                     |
| 84.7354930                        | 0                             | 84.7354930                        | 0                             |
| 84.7955057                        | 0.1307266                     | 85.9994461                        | 1.9497714                     |
| 87.1969784                        | -0.4361305                    | 87.4252746                        | 0                             |
| 87.4252746                        | 0                             | 88.3882899                        | 0.6417239                     |
| 88.8091112                        | 0                             | 88.8091112                        | 0                             |
| 89.5735585                        | 2.2103660                     | 90.7529534                        | 4.4753670                     |
| 91.9266357                        | -1.9099442                    | 92.4918993                        | 0                             |
| 92.4918993                        | 0                             | 93.0947590                        | 1.3057893                     |
| 94.2574700                        | -0.6452860                    | 94.6513440                        | 0                             |
| 94.6513440                        | 0                             | 95.4149085                        | 0.4915215                     |
| 95.8706342                        | 0                             | 95.8706342                        | 0                             |
| 96.5672083                        | 1.5460137                     | 97.7144973                        | 2.8521685                     |
| 98.8311942                        | 0                             | 98.8311942                        | 0                             |
| 98.8568982                        | 0.0903128                     | 99.9945282                        | 2.6914141                     |

## APPENDIX C. GRAPHICS OF DEVIATIONS

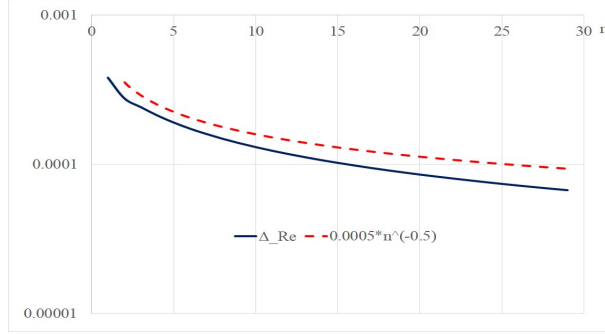


FIGURE 27.  

$$\epsilon_2(n) = \Delta_{Re} = \frac{tr_n - La_{Re}(n)}{La_{Re}(n) - La_{Re}(n-1)}$$

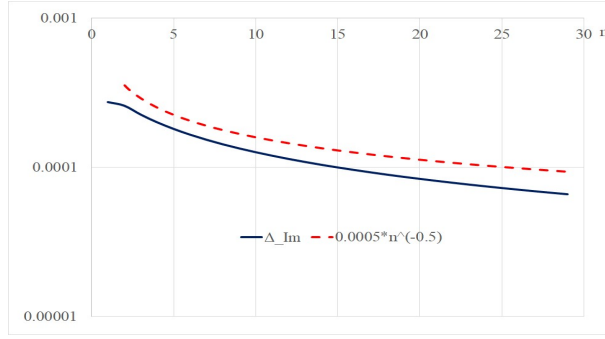


FIGURE 28.  

$$\epsilon_3(n) = \Delta_{Im} = \frac{ti_n - La_{Im}(n)}{La_{Im}(n) - La_{Im}(n-1)}$$

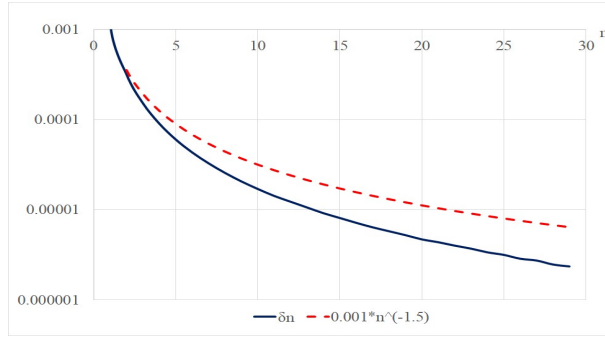


FIGURE 29.  

$$\epsilon_1(n) = \delta_n = -(tr_n - ti_n - (La_{Re}(n) - La_{Im}(n)))$$

Integrating the specific Lambert function's values within the  $\zeta$ -function, we get figures 30 and 31:

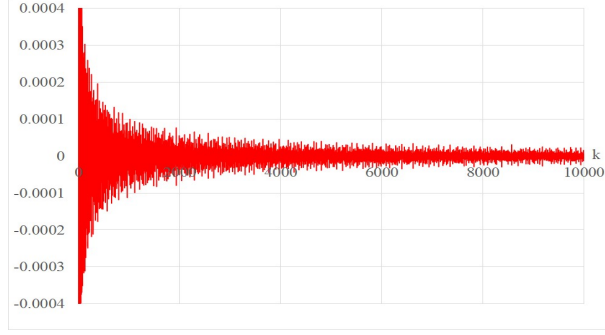


FIGURE 30.  $\Upsilon_{Im}(k) = Im(\zeta(\frac{1}{2} + i\frac{2\pi(k-7/8)}{W(\frac{k-7/8}{e})}))$ ,  
 $k = 1$  to  $10000$ ,  $k \in N$

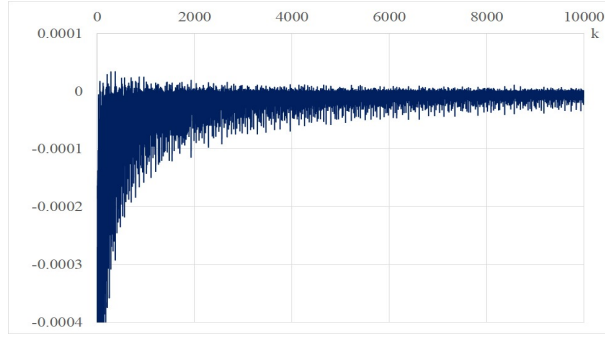


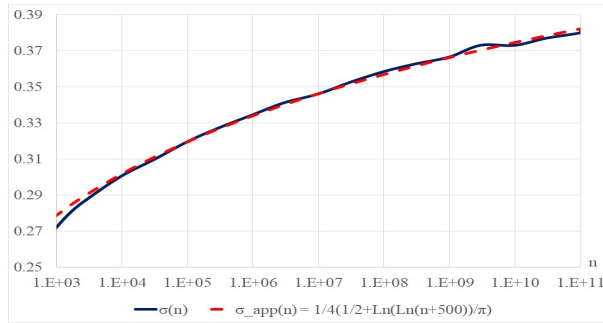
FIGURE 31.  $\Upsilon_{Re}(k) = Re(\zeta(\frac{1}{2} + i\frac{2\pi(k-11/8)}{W(\frac{k-11/8}{e})}))$ ,  
 $k = 1$  to  $10000$ ,  $k \in N$

## APPENDIX D. DATA OF STANDARD DEVIATIONS

The samples are composed of 1000 consecutive elements, starting at  $n$  and the standard deviation is noted  $\sigma(n)$ . The approximation function  $\sigma_{app}(n)$  is equal to  $\frac{1}{4}(\frac{1}{2} + \frac{\text{Ln}(\text{Ln}(n+500))}{\pi})$ . We provide also the relative difference between the two values:  $\Delta r(n) = \frac{\sigma_{app}(n) - \sigma(n)}{\sigma(n)}$ . The two last data are close neighbours showing similarities and also still a notable difference. That is the result of "small" samples.

TABLE 11

| $n$          | $\sigma(n)$ | $\sigma_{app}(n)$ | $\Delta r(n)$ |
|--------------|-------------|-------------------|---------------|
| 1            | 0.2593      | 0.2704            | 4.28 %        |
| 1000         | 0.2790      | 0.2833            | 1.55 %        |
| 3000         | 0.2896      | 0.2921            | 0.83 %        |
| 10000        | 0.3011      | 0.3021            | 0.32 %        |
| 30000        | 0.3096      | 0.3108            | 0.39 %        |
| 100000       | 0.3197      | 0.3195            | -0.06 %       |
| 300000       | 0.3273      | 0.3267            | -0.17 %       |
| 1000000      | 0.3346      | 0.3340            | -0.20 %       |
| 3000000      | 0.3412      | 0.3400            | -0.35 %       |
| 10000000     | 0.3461      | 0.3462            | 0.03 %        |
| 30000000     | 0.3525      | 0.3515            | -0.29 %       |
| 100000000    | 0.3586      | 0.3568            | -0.48 %       |
| 300000000    | 0.3628      | 0.3615            | -0.36 %       |
| 1000000000   | 0.3666      | 0.3662            | -0.11 %       |
| 3000000000   | 0.3732      | 0.3703            | -0.76 %       |
| 10000000000  | 0.3731      | 0.3746            | 0.40 %        |
| 30000000000  | 0.3771      | 0.3783            | 0.33 %        |
| 100000000000 | 0.3801      | 0.3822            | 0.55 %        |
| 100000001000 | 0.3820      | 0.3822            | 0.05 %        |

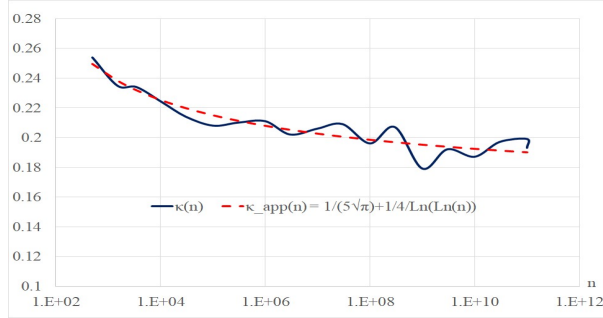
FIGURE 32. Standard deviation  $\sigma$

## APPENDIX E. PROPORTION OF CONSECUTIVE SEQUENCES OF ZEROS

The notion of consecutive sequences has been given in the main text. The samples are composed of  $1000 + 1000$  elements of set 1 and set 2 respectively, starting at  $n$ , and the proportion is labelled  $\kappa(n)$ . The approximation function  $\kappa_{app}(n)$  is equal to  $\frac{1}{5\sqrt{\pi}} + \frac{1}{4 \text{Ln}(\text{Ln}(n+500))}$ . We provide also the relative difference between the two values:  $\Delta r(n) = \frac{\kappa_{app}(n) - \kappa(n)}{\kappa(n)}$ .

TABLE 12

| $n$           | $\kappa$ | $\kappa_{app}(n)$ | $\Delta r(n)$ |
|---------------|----------|-------------------|---------------|
| 1             | 0.254    | 0.2497            | -1.71 %       |
| 1000          | 0.235    | 0.2385            | 1.48 %        |
| 3000          | 0.234    | 0.2319            | -0.89 %       |
| 10000         | 0.224    | 0.2252            | 0.52 %        |
| 30000         | 0.214    | 0.2199            | 2.77 %        |
| 100000        | 0.208    | 0.2151            | 3.43 %        |
| 300000        | 0.210    | 0.2115            | 0.70 %        |
| 1000000       | 0.211    | 0.2080            | -1.40 %       |
| 3000000       | 0.202    | 0.2054            | 1.66 %        |
| 10000000      | 0.206    | 0.2028            | -1.57 %       |
| 30000000      | 0.209    | 0.2007            | -3.98 %       |
| 100000000     | 0.196    | 0.1986            | 1.35 %        |
| 300000000     | 0.207    | 0.1970            | -4.84 %       |
| 1000000000    | 0.179    | 0.1953            | 9.11 %        |
| 3000000000    | 0.192    | 0.1939            | 1.01 %        |
| 10000000000   | 0.187    | 0.1925            | 2.96 %        |
| 30000000000   | 0.197    | 0.1914            | -2.86 %       |
| 100000000000  | 0.199    | 0.1902            | -4.43 %       |
| 1000000001000 | 0.193    | 0.1902            | -1.46 %       |

FIGURE 33.  $\kappa$  evolution

## APPENDIX F. THREE CONSECUTIVE ZEROS

Figure 34 shows the evolution, up to the 50000+50000 zeros, of the pairing by adding 1 each time that a non-trivial zero is reached (by increasing the ordinate) and adding  $-1$  each time a partial zero  $Re(s) = 0$  is met. We observe the systematic rapid return to 0 for the count  $\#(ad)$ . We mention in table 13 the number of times  $\#\#(ad)$  some value of  $\#(ad)$  is obtained in this data collection.

TABLE 13

|            |    |       |       |       |   |
|------------|----|-------|-------|-------|---|
| $\#(ad)$   | -2 | -1    | 0     | 1     | 2 |
| $\#\#(ad)$ | 5  | 24982 | 49993 | 25018 | 2 |

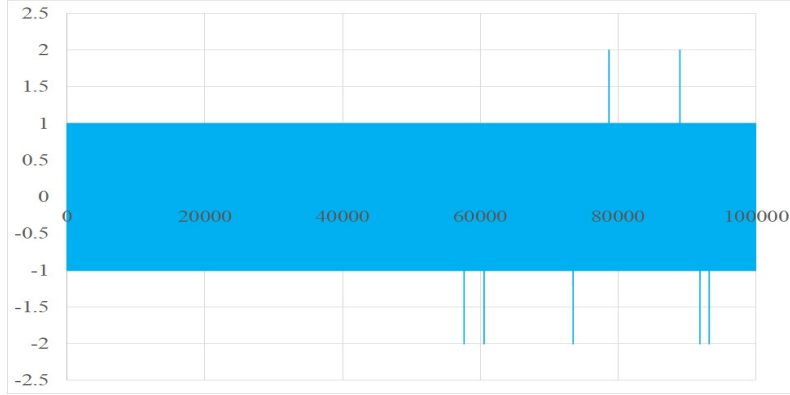
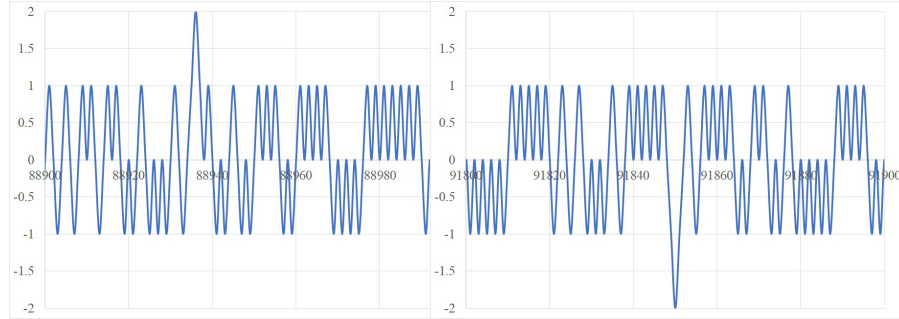

 FIGURE 34. Pairing: Evolution of  $\#(ad)$ 

 FIGURE 35.  
 Paring: Evolution of  $\#(ad)$ 

 (A) Detail for some temporary  
 $\#(ad) = 2$ 

 (B) Detail for some temporary  
 $\#(ad) = -2$

TABLE 14

| <i>type</i> | <i>n</i>            | <i>n</i>            | <i>n</i>            |
|-------------|---------------------|---------------------|---------------------|
| re          | 39324               | 44467               | 45926               |
| ri          | 39324               | 44467               | 45925               |
| ri          | 39325               | 44468               | 45926               |
| ri          | 39326               | 44469               | 45927               |
| re          | 39325               | 44468               | 45927               |
| <i>type</i> | <i>ordinates</i>    | <i>ordinates</i>    | <i>ordinates</i>    |
| re          | 32694.0584          | 36446.1498          | 37502.2671          |
| ri          | 32694.1706          | 36446.1535          | 37502.3231          |
| ri          | 32694.5156          | 36446.7618          | 37502.535           |
| ri          | 32694.7693          | 36446.8685          | 37502.8381          |
| re          | 32694.7927          | 36446.8748          | 37502.9898          |
|             | <i>spacings</i>     | <i>spacings</i>     | <i>spacings</i>     |
|             | 0.1122              | 0.0038              | 0.0559              |
|             | 0.345               | 0.6083              | 0.2119              |
|             | 0.2537              | 0.1067              | 0.3031              |
|             | 0.0234              | 0.0063              | 0.1518              |
|             | <i>totalspacing</i> | <i>totalspacing</i> | <i>totalspacing</i> |
|             | 0.7343              | 0.7251              | 0.7227              |

TABLE 15.  
 $lag\_n = 10^{21} + 1$ ,  
 $lag\_t = 1.44176897509546973000 \cdot 10^{20}$ .

| <i>type</i> | $n - lag\_n$         | $n - lag\_n$         | $n - lag\_n$         | $n - lag\_n$         | $n - lag\_n$         |
|-------------|----------------------|----------------------|----------------------|----------------------|----------------------|
| re          | 119                  | 135                  | 792                  | 1210                 | 1311                 |
| ri          | 120                  | 135                  | 793                  | 1209                 | 1311                 |
| ri          | 120                  | 136                  | 793                  | 1210                 | 1312                 |
| ri          | 121                  | 136                  | 794                  | 1211                 | 1312                 |
| re          | 121                  | 137                  | 794                  | 1211                 | 1313                 |
| <i>type</i> | $t - lag\_t$         | $t - lag\_t$         | $t - lag\_t$         | $t - lag\_t$         | $t - lag\_t$         |
| re          | 555.2929             | 557.407              | 650.1474             | 708.9205             | 723.1557             |
| ri          | 555.2998             | 557.4186             | 650.15               | 708.9393             | 723.1806             |
| ri          | 555.3471             | 557.4616             | 650.179              | 709.0054             | 723.2689             |
| ri          | 555.4214             | 557.5318             | 650.2569             | 709.0563             | 723.2966             |
| re          | 555.4338             | 557.548              | 650.2883             | 709.0614             | 723.2967             |
|             | <i>spacings</i>      | <i>spacings</i>      | <i>spacings</i>      | <i>spacings</i>      | <i>spacings</i>      |
|             | 0.0069               | 0.0116               | 0.0027               | 0.0188               | 0.0249               |
|             | 0.0474               | 0.043                | 0.0289               | 0.066                | 0.0884               |
|             | 0.0743               | 0.0701               | 0.078                | 0.0509               | 0.0277               |
|             | 0.0124               | 0.0162               | 0.0314               | 0.0052               | 0                    |
|             | <i>totalspacings</i> | <i>totalspacings</i> | <i>totalspacings</i> | <i>totalspacings</i> | <i>totalspacings</i> |
|             | 0.1409               | 0.1409               | 0.1409               | 0.1409               | 0.1409               |

TABLE 16.  
 $lag\_n = 10^{21} + 1$ ,  
 $lag\_t = 1.44176897509546973000 \cdot 10^{20}$ .

| <i>type</i> | $n - lag\_n$         | $n - lag\_n$         | $n - lag\_n$         | $n - lag\_n$         | $n - lag\_n$         |
|-------------|----------------------|----------------------|----------------------|----------------------|----------------------|
| re          | 1859                 | 1877                 | 2039                 | 2520                 | 2703                 |
| ri          | 1860                 | 1877                 | 2039                 | 2520                 | 2704                 |
| ri          | 1860                 | 1878                 | 2040                 | 2521                 | 2704                 |
| ri          | 1861                 | 1878                 | 2040                 | 2521                 | 2705                 |
| re          | 1861                 | 1879                 | 2041                 | 2522                 | 2705                 |
| <i>type</i> | $t - lag\_t$         | $t - lag\_t$         | $t - lag\_t$         | $t - lag\_t$         | $t - lag\_t$         |
| re          | 800.5333             | 802.9293             | 825.762              | 893.5555             | 919.489              |
| ri          | 800.5547             | 802.9301             | 825.8046             | 893.5681             | 919.5006             |
| ri          | 800.5769             | 802.9997             | 825.8683             | 893.628              | 919.5866             |
| ri          | 800.6554             | 803.0679             | 825.8956             | 893.6816             | 919.6161             |
| re          | 800.6742             | 803.0703             | 825.903              | 893.6965             | 919.6299             |
|             | <i>spacings</i>      | <i>spacings</i>      | <i>spacings</i>      | <i>spacings</i>      | <i>spacings</i>      |
|             | 0.0214               | 0.0007               | 0.0426               | 0.0126               | 0.0117               |
|             | 0.0223               | 0.0696               | 0.0637               | 0.0599               | 0.0859               |
|             | 0.0785               | 0.0682               | 0.0273               | 0.0536               | 0.0295               |
|             | 0.0188               | 0.0024               | 0.0074               | 0.0149               | 0.0139               |
|             | <i>totalspacings</i> | <i>totalspacings</i> | <i>totalspacings</i> | <i>totalspacings</i> | <i>totalspacings</i> |
|             | 0.1409               | 0.1409               | 0.1409               | 0.1409               | 0.1409               |

TABLE 17.  
 $lag\_n = 10^{21} + 1$ ,  
 $lag\_t = 1.44176897509546973000 \cdot 10^{20}$ .

| <i>type</i> | $n - lag\_n$         | $n - lag\_n$         | $n - lag\_n$         | $n - lag\_n$         | $n - lag\_n$         |
|-------------|----------------------|----------------------|----------------------|----------------------|----------------------|
| re          | 3417                 | 6465                 | 6665                 | 6845                 | 7381                 |
| ri          | 3417                 | 6465                 | 6665                 | 6845                 | 7382                 |
| ri          | 3418                 | 6466                 | 6666                 | 6846                 | 7382                 |
| ri          | 3418                 | 6466                 | 6666                 | 6846                 | 7383                 |
| re          | 3419                 | 6467                 | 6667                 | 6847                 | 7383                 |
| <i>type</i> | $t - lag\_t$         | $t - lag\_t$         | $t - lag\_t$         | $t - lag\_t$         | $t - lag\_t$         |
| re          | 1019.9812            | 1449.5747            | 1477.7632            | 1503.1329            | 1578.8192            |
| ri          | 1020                 | 1449.5943            | 1477.7751            | 1503.1397            | 1578.8232            |
| ri          | 1020.0296            | 1449.6929            | 1477.8436            | 1503.1841            | 1578.8685            |
| ri          | 1020.1185            | 1449.7057            | 1477.9003            | 1503.2356            | 1578.9558            |
| re          | 1020.1221            | 1449.7156            | 1477.9042            | 1503.2739            | 1578.9601            |
|             | <i>spacings</i>      | <i>spacings</i>      | <i>spacings</i>      | <i>spacings</i>      | <i>spacings</i>      |
|             | 0.0189               | 0.0196               | 0.0118               | 0.0068               | 0.004                |
|             | 0.0296               | 0.0986               | 0.0685               | 0.0444               | 0.0454               |
|             | 0.0889               | 0.0128               | 0.0566               | 0.0515               | 0.0872               |
|             | 0.0036               | 0.0099               | 0.0039               | 0.0383               | 0.0044               |
|             | <i>totalspacings</i> | <i>totalspacings</i> | <i>totalspacings</i> | <i>totalspacings</i> | <i>totalspacings</i> |
|             | 0.1409               | 0.1409               | 0.1409               | 0.1409               | 0.1409               |

TABLE 18.  
 $lag\_n = 10^{21} + 1$ ,  
 $lag\_t = 1.44176897509546973000 \cdot 10^{20}$ .

| <i>type</i> | $n - lag\_n$         | $n - lag\_n$         | $n - lag\_n$         | $n - lag\_n$         | $n - lag\_n$         |
|-------------|----------------------|----------------------|----------------------|----------------------|----------------------|
| re          | 7413                 | 7745                 | 8587                 | 8766                 | 9661                 |
| ri          | 7414                 | 7745                 | 8587                 | 8766                 | 9661                 |
| ri          | 7414                 | 7746                 | 8588                 | 8767                 | 9662                 |
| ri          | 7415                 | 7746                 | 8588                 | 8767                 | 9662                 |
| re          | 7415                 | 7747                 | 8589                 | 8768                 | 9663                 |
| <i>type</i> | $t - lag\_t$         | $t - lag\_t$         | $t - lag\_t$         | $t - lag\_t$         | $t - lag\_t$         |
| re          | 1583.3294            | 1629.9814            | 1748.6552            | 1773.884             | 1900.0278            |
| ri          | 1583.3401            | 1629.9948            | 1748.6562            | 1773.8977            | 1900.0659            |
| ri          | 1583.4421            | 1630.0423            | 1748.7048            | 1773.9784            | 1900.0998            |
| ri          | 1583.4693            | 1630.111             | 1748.7801            | 1774.0111            | 1900.1661            |
| re          | 1583.4703            | 1630.1224            | 1748.7962            | 1774.0249            | 1900.1687            |
|             | <i>spacings</i>      | <i>spacings</i>      | <i>spacings</i>      | <i>spacings</i>      | <i>spacings</i>      |
|             | 0.0107               | 0.0134               | 0.001                | 0.0137               | 0.0382               |
|             | 0.102                | 0.0475               | 0.0487               | 0.0807               | 0.0338               |
|             | 0.0272               | 0.0687               | 0.0753               | 0.0328               | 0.0663               |
|             | 0.001                | 0.0114               | 0.016                | 0.0138               | 0.0026               |
|             | <i>totalspacings</i> | <i>totalspacings</i> | <i>totalspacings</i> | <i>totalspacings</i> | <i>totalspacings</i> |
|             | 0.1409               | 0.1409               | 0.1409               | 0.1409               | 0.1409               |

TABLE 19.  
 $lag\_n = 10^{22} + 1$ ,  
 $lag\_t = 1.370919909931995300000 \cdot 10^{21}$ .

|    | $n - lag\_n$         | $n - lag\_n$         | $n - lag\_n$         | $n - lag\_n$         | $n - lag\_n$         |
|----|----------------------|----------------------|----------------------|----------------------|----------------------|
| re | 215                  | 1193                 | 3828                 | 3881                 | 4899                 |
| ri | 216                  | 1193                 | 3829                 | 3882                 | 4899                 |
| ri | 216                  | 1194                 | 3829                 | 3882                 | 4900                 |
| ri | 217                  | 1194                 | 3830                 | 3883                 | 4900                 |
| re | 217                  | 1195                 | 3830                 | 3883                 | 4901                 |
|    | $t - lag\_t$         | $t - lag\_t$         | $t - lag\_t$         | $t - lag\_t$         | $t - lag\_t$         |
| re | 8255.6156            | 8386.6945            | 8740.3526            | 8747.4633            | 8883.9088            |
| ri | 8255.6317            | 8386.6989            | 8740.3693            | 8747.4721            | 8883.9101            |
| ri | 8255.6595            | 8386.7573            | 8740.4315            | 8747.5558            | 8884.0109            |
| ri | 8255.7033            | 8386.8156            | 8740.4694            | 8747.5766            | 8884.0413            |
| re | 8255.7498            | 8386.8287            | 8740.4867            | 8747.5975            | 8884.0429            |
|    | <i>spacings</i>      | <i>spacings</i>      | <i>spacings</i>      | <i>spacings</i>      | <i>spacings</i>      |
|    | 0.0161               | 0.0044               | 0.0167               | 0.0087               | 0.0013               |
|    | 0.0278               | 0.0584               | 0.0622               | 0.0838               | 0.1008               |
|    | 0.0438               | 0.0583               | 0.0379               | 0.0207               | 0.0304               |
|    | 0.0465               | 0.013                | 0.0174               | 0.0209               | 0.0016               |
|    | <i>totalspacings</i> | <i>totalspacings</i> | <i>totalspacings</i> | <i>totalspacings</i> | <i>totalspacings</i> |
|    | 0.1342               | 0.1342               | 0.1342               | 0.1342               | 0.1342               |

TABLE 20.  
 $lag\_n = 10^{22} + 1$ ,  
 $lag\_t = 1.370919909931995300000 \cdot 10^{21}$ .

|    | $n - lag\_n$    | $n - lag\_n$    | $n - lag\_n$    | $n - lag\_n$    | $n - lag\_n$    |
|----|-----------------|-----------------|-----------------|-----------------|-----------------|
| re | 5265            | 5850            | 6308            | 7423            | 7480            |
| ri | 5265            | 5851            | 6309            | 7423            | 7480            |
| ri | 5266            | 5851            | 6309            | 7424            | 7481            |
| ri | 5266            | 5852            | 6310            | 7424            | 7481            |
| re | 5267            | 5852            | 6310            | 7425            | 7482            |
|    | $t - lag\_t$    | $t - lag\_t$    | $t - lag\_t$    | $t - lag\_t$    | $t - lag\_t$    |
| re | 8933.013        | 9011.6335       | 9073.081        | 9222.5404       | 9230.1878       |
| ri | 8933.0147       | 9011.6515       | 9073.0933       | 9222.548        | 9230.2155       |
| ri | 8933.1088       | 9011.684        | 9073.1475       | 9222.6183       | 9230.2712       |
| ri | 8933.1423       | 9011.7486       | 9073.1932       | 9222.6729       | 9230.3204       |
| re | 8933.1472       | 9011.7677       | 9073.2151       | 9222.6746       | 9230.322        |
|    | $spacings$      | $spacings$      | $spacings$      | $spacings$      | $spacings$      |
|    | 0.0017          | 0.018           | 0.0124          | 0.0076          | 0.0277          |
|    | 0.0941          | 0.0325          | 0.0542          | 0.0703          | 0.0558          |
|    | 0.0335          | 0.0646          | 0.0457          | 0.0546          | 0.0491          |
|    | 0.0049          | 0.0191          | 0.0219          | 0.0017          | 0.0016          |
|    | $totalspacings$ | $totalspacings$ | $totalspacings$ | $totalspacings$ | $totalspacings$ |
|    | 0.1342          | 0.1342          | 0.1342          | 0.1342          | 0.1342          |

TABLE 21.  
 $lag\_n = 10^{22} + 1$ ,  
 $lag\_t = 1.370919909931995300000 \cdot 10^{21}$ .

|    | $n - lag\_n$         | $n - lag\_n$         | $n - lag\_n$         | $n - lag\_n$         | $n - lag\_n$         |
|----|----------------------|----------------------|----------------------|----------------------|----------------------|
| re | 7883                 | 8054                 | 8478                 | 8550                 | 8577                 |
| ri | 7883                 | 8055                 | 8479                 | 8551                 | 8577                 |
| ri | 7884                 | 8055                 | 8479                 | 8551                 | 8578                 |
| ri | 7884                 | 8056                 | 8480                 | 8552                 | 8578                 |
| re | 7885                 | 8056                 | 8480                 | 8552                 | 8579                 |
|    | $t - lag\_t$         | $t - lag\_t$         | $t - lag\_t$         | $t - lag\_t$         | $t - lag\_t$         |
| re | 9284.2562            | 9307.3325            | 9364.2183            | 9373.8782            | 9377.3664            |
| ri | 9284.2841            | 9307.3417            | 9364.2363            | 9373.896             | 9377.3796            |
| ri | 9284.3431            | 9307.4163            | 9364.2611            | 9373.9474            | 9377.4451            |
| ri | 9284.3841            | 9307.4398            | 9364.3396            | 9373.9992            | 9377.4735            |
| re | 9284.3903            | 9307.4666            | 9364.3525            | 9374.0123            | 9377.5006            |
|    | <i>spacings</i>      | <i>spacings</i>      | <i>spacings</i>      | <i>spacings</i>      | <i>spacings</i>      |
|    | 0.028                | 0.0092               | 0.018                | 0.0179               | 0.0132               |
|    | 0.0589               | 0.0746               | 0.0248               | 0.0514               | 0.0655               |
|    | 0.0411               | 0.0234               | 0.0785               | 0.0518               | 0.0284               |
|    | 0.0062               | 0.0269               | 0.0128               | 0.0131               | 0.0271               |
|    | <i>totalspacings</i> | <i>totalspacings</i> | <i>totalspacings</i> | <i>totalspacings</i> | <i>totalspacings</i> |
|    | 0.1342               | 0.1342               | 0.1342               | 0.1342               | 0.1342               |

## APPENDIX G. PARI GP PROGRAMS

Frame alternative approximative imaginary value' positions.  
on the critical line

```
{a = 11/8; for(k = 0, 30,
print(k" "real(2*Pi*(k-a)/lambertw((k-a)/exp(1))))})
```

Proximity to target 0 with alternative frame.

```
{print("Set 2: Re(zeta(s)) = 0");
a = 11/8; for(k = 1000, 1015,
print(k" "real(zeta(1/2+I*2*Pi*(k-a)/lambertw((k-a)/exp(1))))))}
{print("Set 3: Im(zeta(s)) = 0");
a = 7/8; for(k = 1000, 1015,
print(k" "imag(zeta(1/2+I*2*Pi*(k-a)/lambertw((k-a)/exp(1))))))}
```

Plotting curves.

```
{sigma1 = 0.5; sigma2 = -5; export(sigma1, sigma2);
parplot(t = 37500.7, 37502.9,
[(2.5*(t^(-1/2+ sigma1*(1-1.83806/log(t)))))*real(zeta(sigma1+I*t)),
(2.5*(t^(-1/2+ sigma2*(1-1.83806/log(t)))))*real(zeta(sigma2+I*t))])}
```

Plotting approximative first derivatives.

```
{epsil1 = 0.00001; epsil2 = 0.00001*I; delt = 0.05;
export(epsil1, epsil2, delt);
parplot(t = 0.2, 21,
[(zeta(0.5-delt+epsil1+I*t)-zeta(0.5-delt+I*t))/epsil1,
(zeta(0.5+delt+epsil2+I*t)-zeta(0.5+delt+I*t))/epsil2],
"Complex")}
```

Plotting approximative second derivatives.

```
{epsil1 = 0.00001; epsil2 = 0.00001*I; delt = 0.05;
export(epsil1, epsil2, delt);
parplot(t = 0.9, 23.5,
[(zeta(0.5-delt+epsil1+I*t)-2*zeta(0.5-delt+I*t)+zeta(0.5-delt-epsil1+I*t))/epsil1/epsil1,
(zeta(0.5+delt+epsil2+I*t)-2*zeta(0.5+delt+I*t)+zeta(0.5+delt-epsil2+I*t))/epsil2/epsil2],
"Complex")}
```

Note that the quotes have to be converted into straight quotes on the Pari gp browser. The exponentiation sign ^ has also to be corrected.

## LITERATURE AND SOURCES

- [1] Bernhard Riemann. Ueber die Anzahl der Primzahlen unter einer gegebenen Grosse. Monatsberichte der Berliner Akademie. Nov 1859.
- [2] Luis Báez-Duarte. Fast proof of functional equation for  $\zeta(s)$ . 14 May 2003 (arXiv math/0305191).
- [3] Tom M. Apóstol. Formulas for higher derivatives of the Riemann Zeta function Mathematics of computation. Vol 44, Num 169. Jan. 1985, p 223-232.
- [4] Harold Davenport. Multiplicative Number Theory. Chapter 15. Graduate Texts in Mathematics. Springer.
- [5] <https://mathoverflow.net/questions/407392/riemann-von-mangoldt-formula>
- [6] 3Blue1Brown. Visualizing the Riemann zeta function and analytic continuation. <https://www.youtube.com/watch?v=sD0NjbwqLYw>
- [7] Database of L-functions, modular forms, and related objects. <https://www.lmfdb.org/zeros/zeta/>
- [8] Andrew M. Odlyzko home page <https://www-users.cse.umn.edu/~odlyzko/>
- [9] [https://en.wikipedia.org/wiki/Riemann\\_hypothesis](https://en.wikipedia.org/wiki/Riemann_hypothesis)
- [10] [https://en.wikipedia.org/wiki/Riemann\\_zeta\\_function](https://en.wikipedia.org/wiki/Riemann_zeta_function)
- [11] [https://en.wikipedia.org/wiki/Abel-Plana\\_formula](https://en.wikipedia.org/wiki/Abel-Plana_formula)
- [12] [https://en.wikipedia.org/wiki/Lambert\\_W\\_function](https://en.wikipedia.org/wiki/Lambert_W_function)
- [13] [https://en.wikipedia.org/wiki/Riemann-Von\\_Mangoldt\\_formula](https://en.wikipedia.org/wiki/Riemann-Von_Mangoldt_formula)
- [14] [https://en.wikipedia.org/wiki/Normal\\_distribution](https://en.wikipedia.org/wiki/Normal_distribution)
- [15] [https://en.wikipedia.org/wiki/Conformal\\_map](https://en.wikipedia.org/wiki/Conformal_map)
- [16] [https://en.wikipedia.org/wiki/Zeros\\_and\\_poles](https://en.wikipedia.org/wiki/Zeros_and_poles)  
[https://fr.wikipedia.org/wiki/Zéro\\_d'une\\_fonction\\_holomorphe](https://fr.wikipedia.org/wiki/Zéro_d'une_fonction_holomorphe)
- [17] <https://hubertschaetzel.wixsite.com/website>

INPG GRENOBLE

 Email address: `hubert.schaetzel@wanadoo.fr`

 URL: <https://hubertschaetzel.wixsite.com/website>